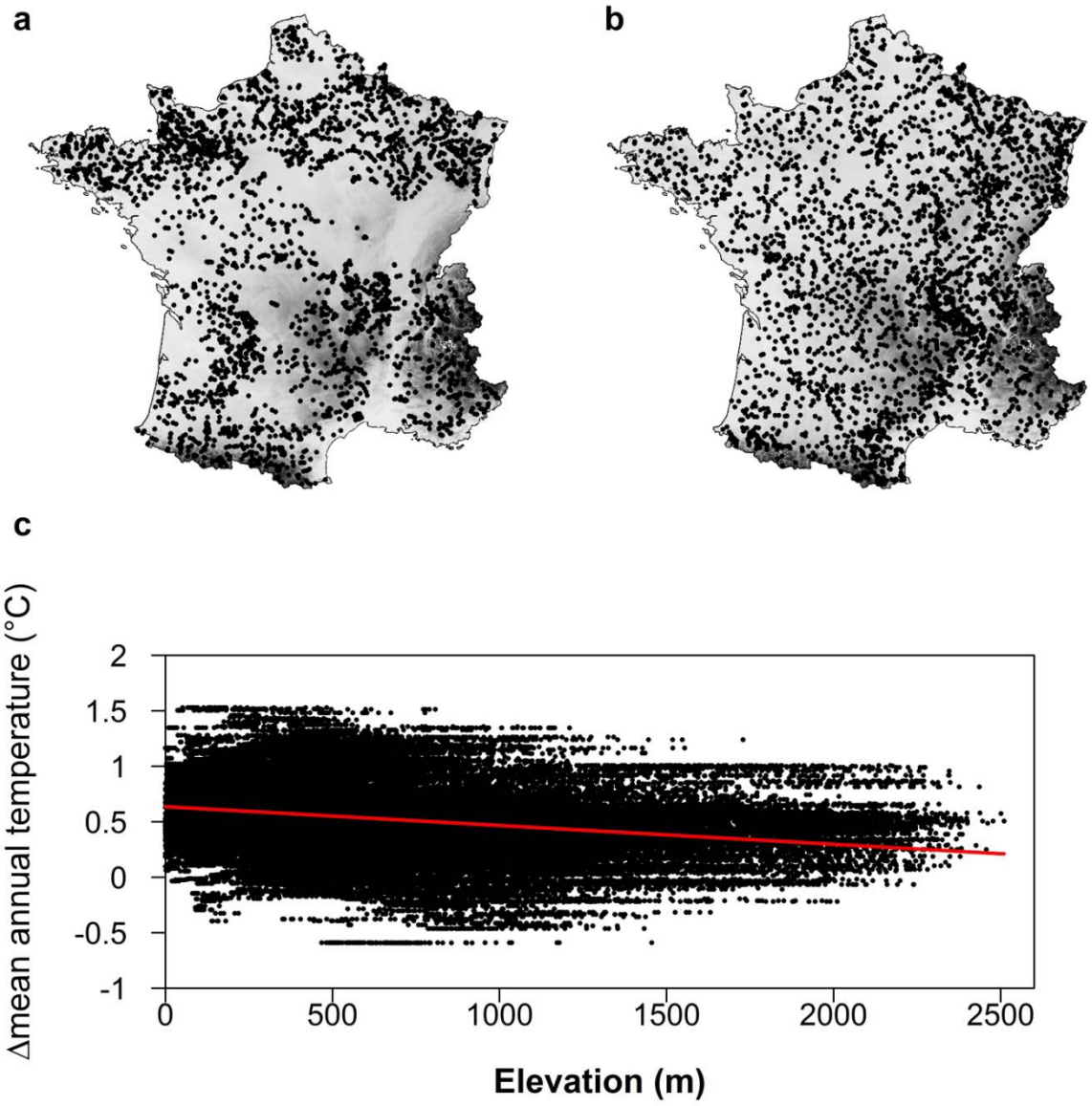


**Supplementary Figure 1 | Spatial distribution and climatic conditions of the sampling sites**. Spatial distribution of the sites in the (**a**) 1980-1992 ($n$ = 3549), and (**b**) 2003-09 ($n$ = 3543) periods with the grey scale illustrating the altitudinal gradient across France. (**c**) Red line is the linear regression of the changes in mean annual water temperature across the French hydrographic network between the two time periods as a function of the altitudinal gradient ($p < 0.001$, $n$ = 100,888 stream reaches).

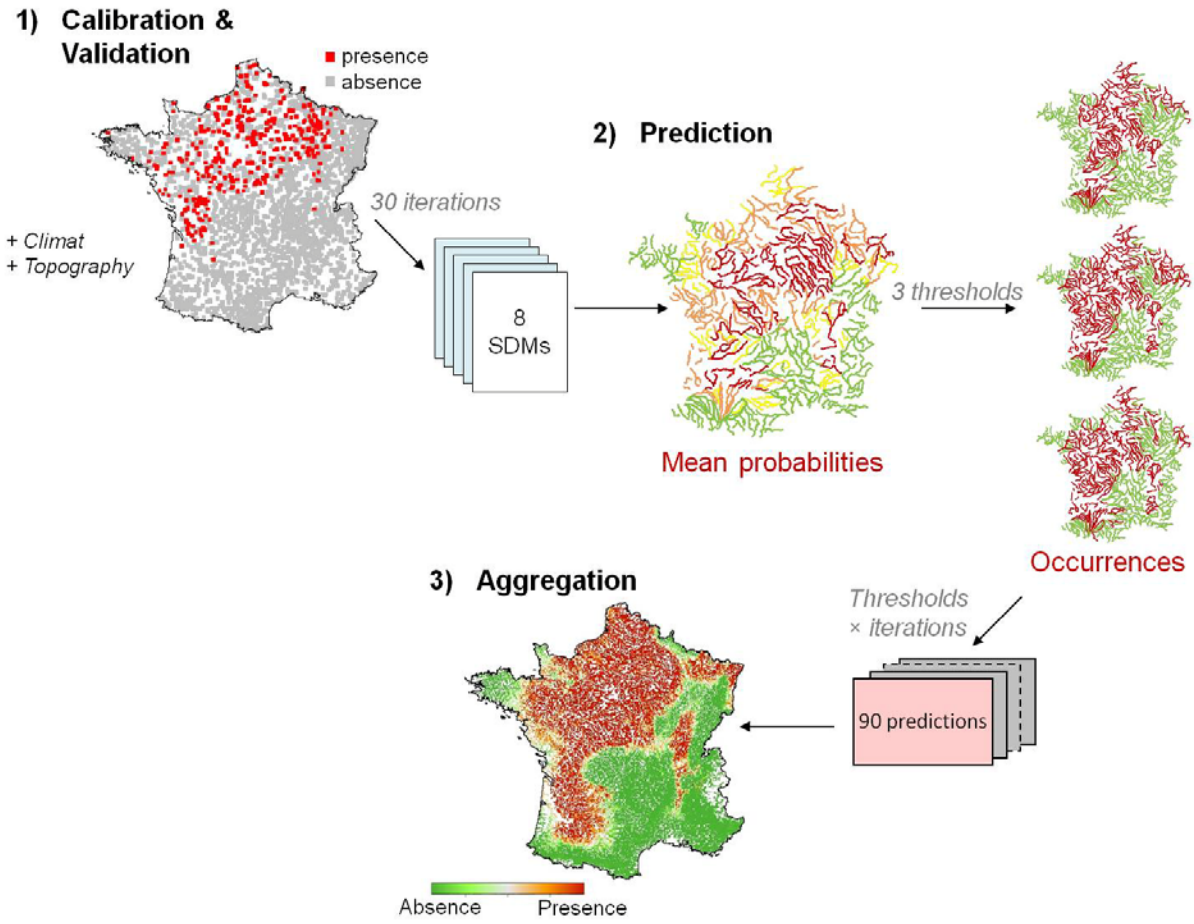


**Supplementary Figure 2 | Different steps of the modelling process.** The description is given for one species and one time period[1] (see Supplementary Methods for details).

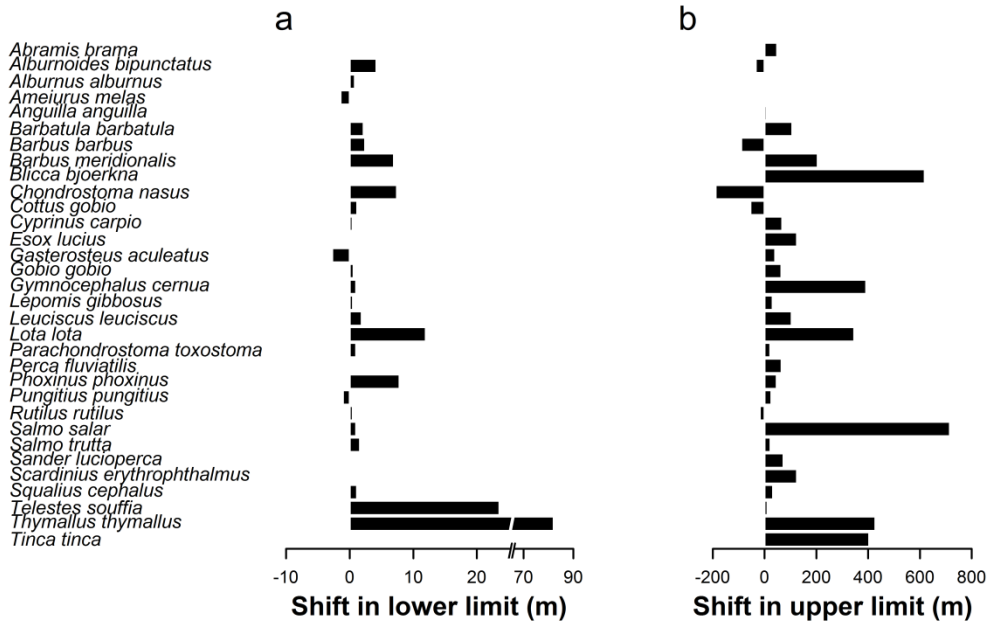


**Supplementary Figure 3 | Rates of range shift for the 32 studied species**: (**a**) lower and (**b**) upper altitudinal limit.

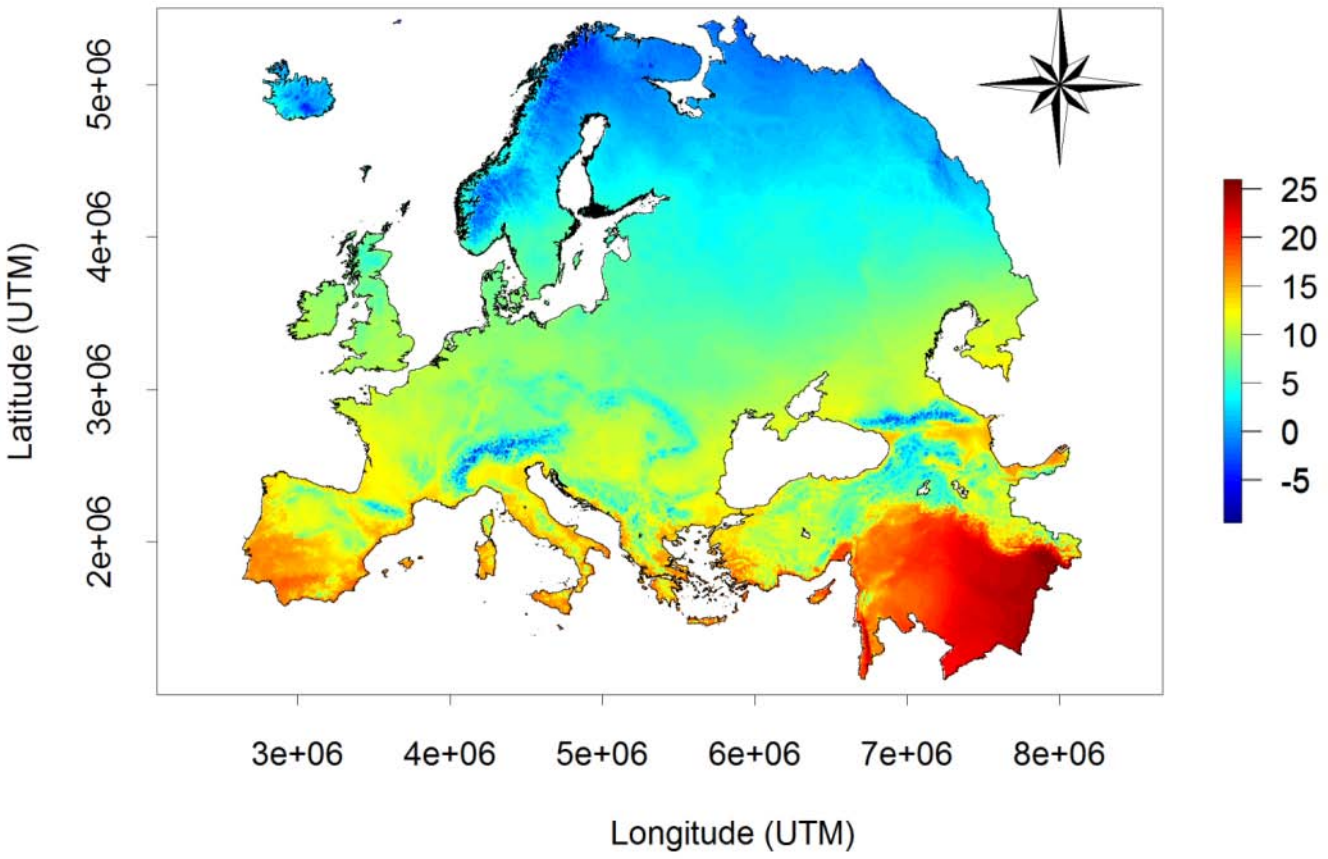


**Supplementary Figure 4 | Climatic gradient across Europe**. Mean annual surface temperature (°C) across Europe (resolution: 30 arc-s) for the 1960-90 period (BIOCLIM[2]).

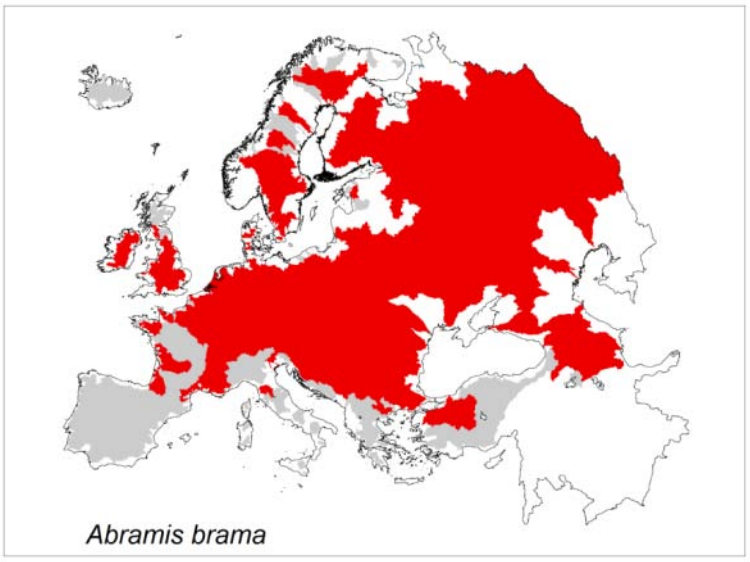
Abramis brama

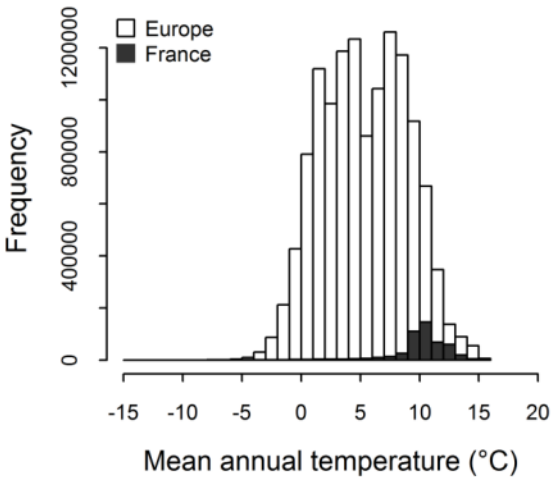
Europe
France
Frequency
0
400000
800000
1200000
-15
-10
-5
0
5
10
15
20
Mean annual temperature (°C)

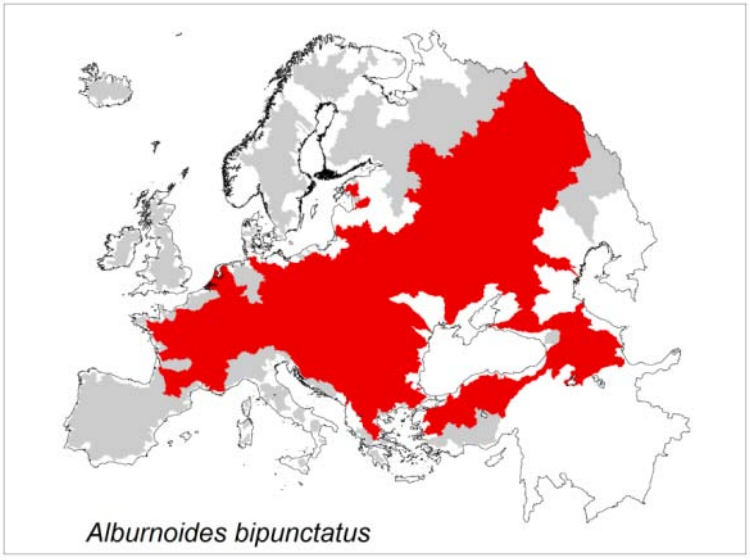
Alburnoides bipunctatus

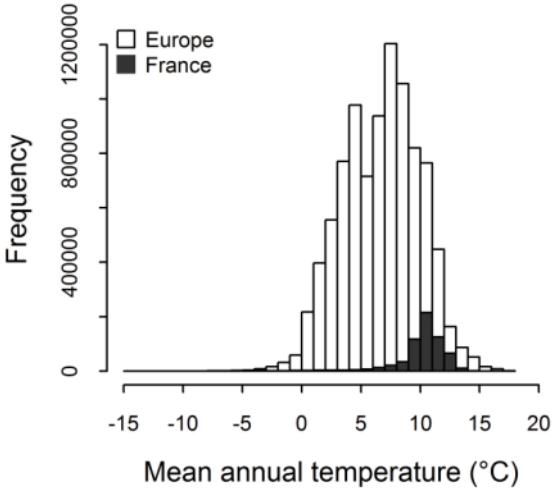
Europe
France
Frequency
0
400000
800000
1200000
-15
-10
-5
0
5
10
15
20
Mean annual temperature (°C)

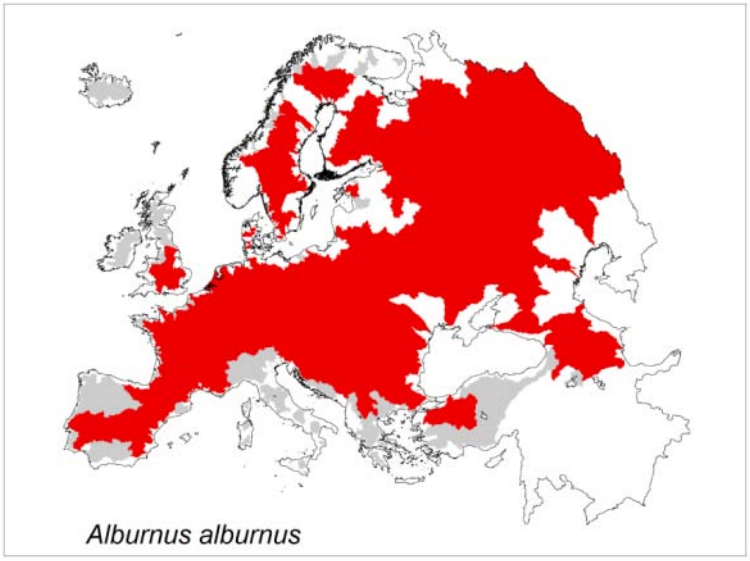
Alburnus alburnus

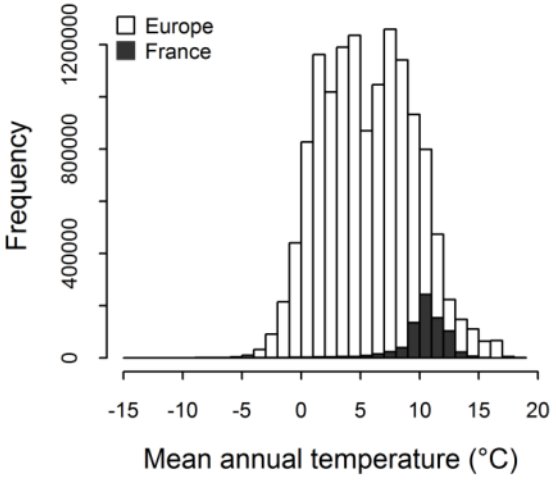
Europe
France
Frequency
0
400000
800000
1200000
-15
-10
-5
0
5
10
15
20
Mean annual temperature (°C)

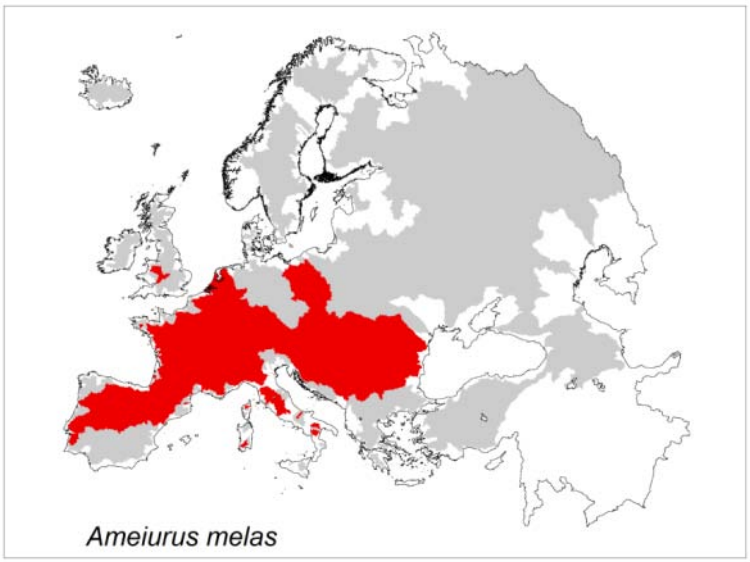
Ameiurus melas

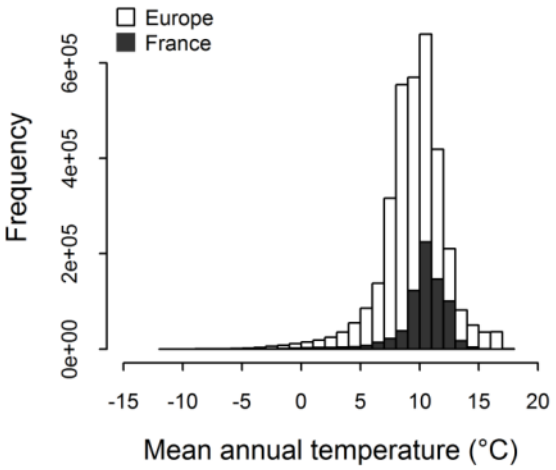
Europe
France
Frequency
0e+00
2e+05
4e+05
6e+05
-15
-10
-5
0
5
10
15
20
Mean annual temperature (°C)

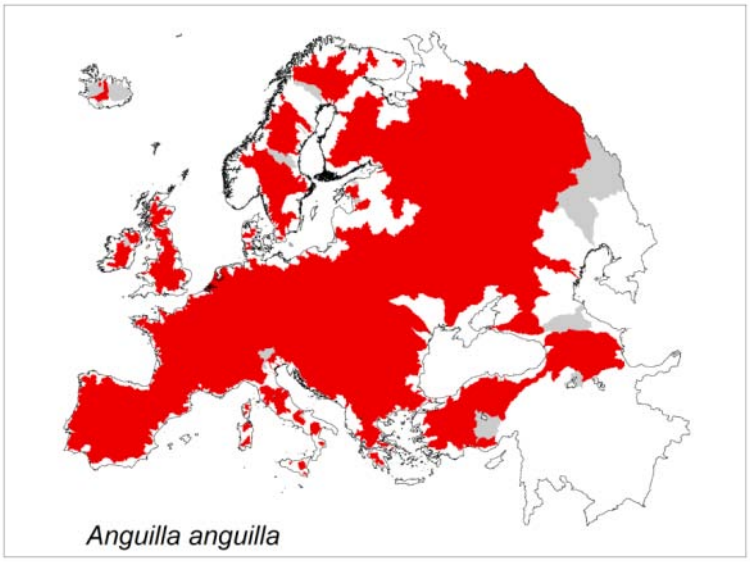
Anguilla anguilla

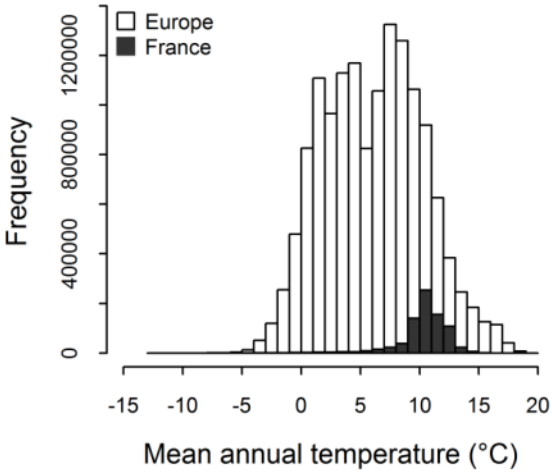
Europe
France
Frequency
0
400000
800000
1200000
-15
-10
-5
0
5
10
15
20
Mean annual temperature (°C)

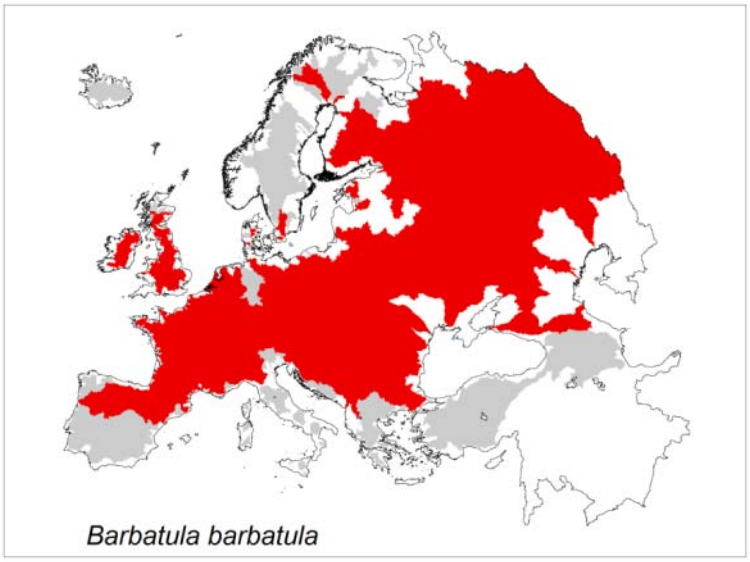
Barbatula barbatula

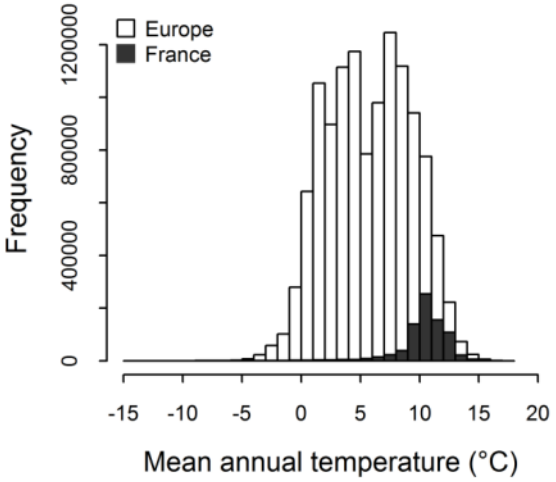
Europe
France
Frequency
0
400000
800000
1200000
-15
-10
-5
0
5
10
15
20
Mean annual temperature (°C)

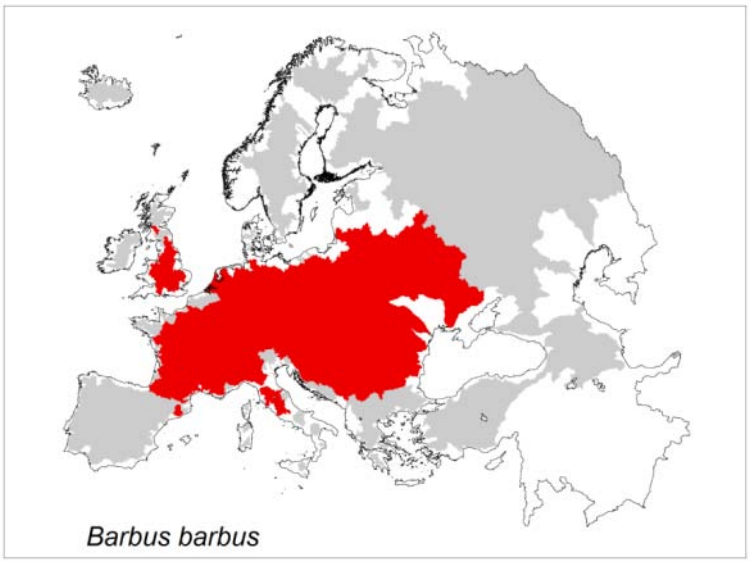
Barbus barbus

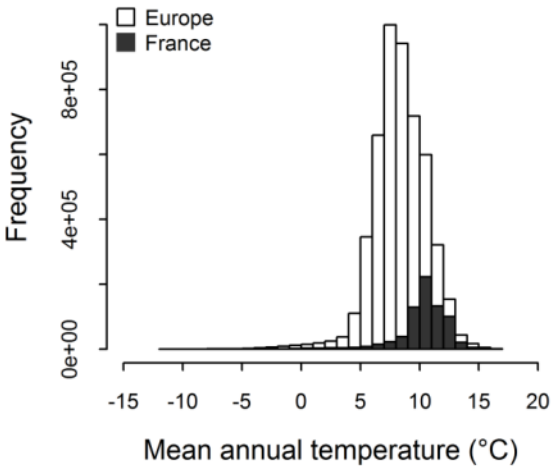
Europe
France
Frequency
0e+00
4e+05
8e+05
-15
-10
-5
0
5
10
15
20
Mean annual temperature (°C)

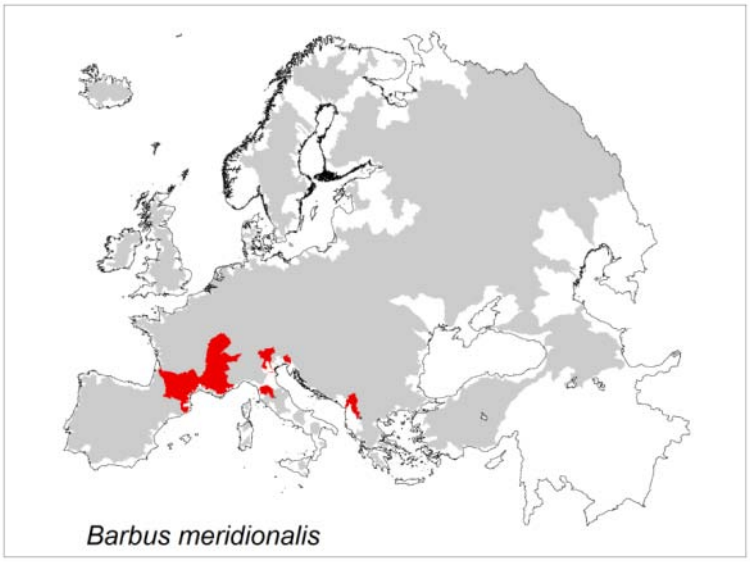
Barbus meridionalis

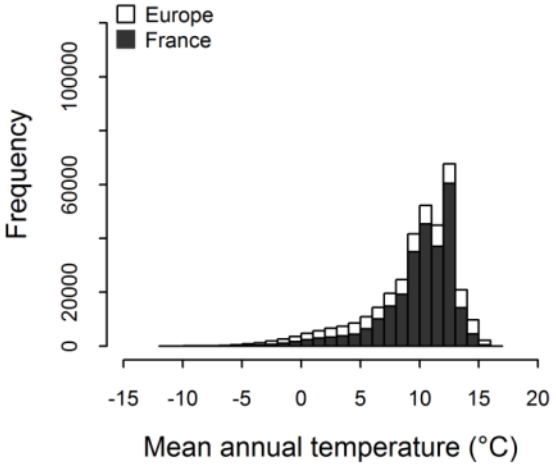
Europe
France
Frequency
0
20000
60000
100000
-15
-10
-5
0
5
10
15
20
Mean annual temperature (°C)


Blicca bjoerkna

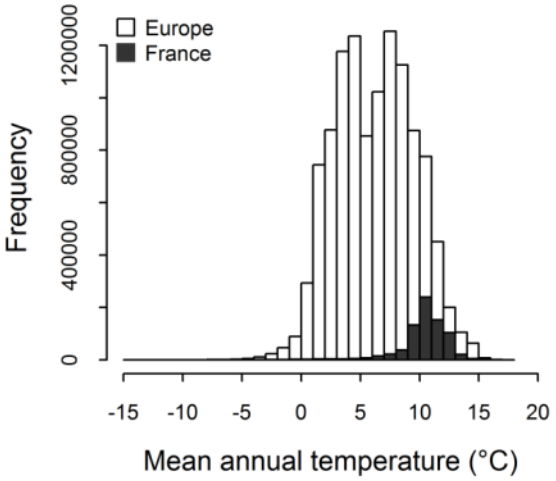
Europe
France
Frequency
0
400000
800000
1200000
-15
-10
-5
0
5
10
15
20
Mean annual temperature (°C)

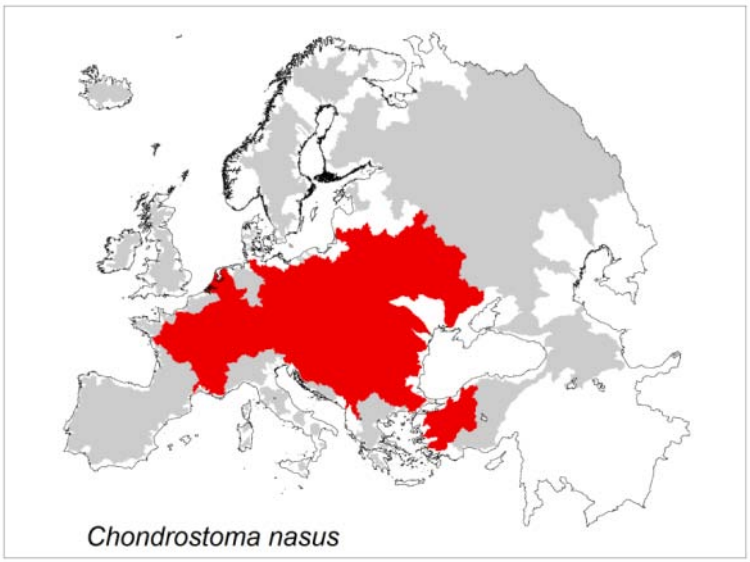
Chondrostoma nasus

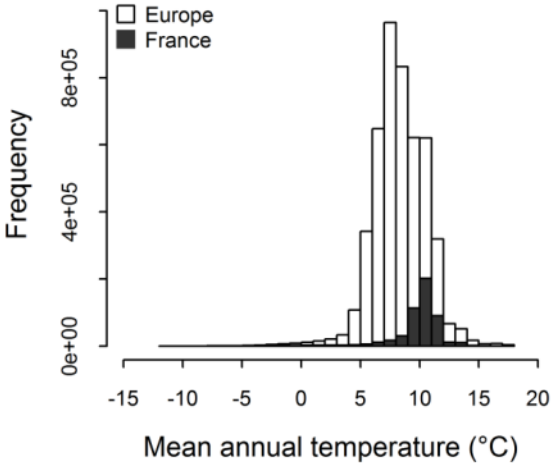
Europe
France
Frequency
0e+00
4e+05
8e+05
-15
-10
-5
0
5
10
15
20
Mean annual temperature (°C)

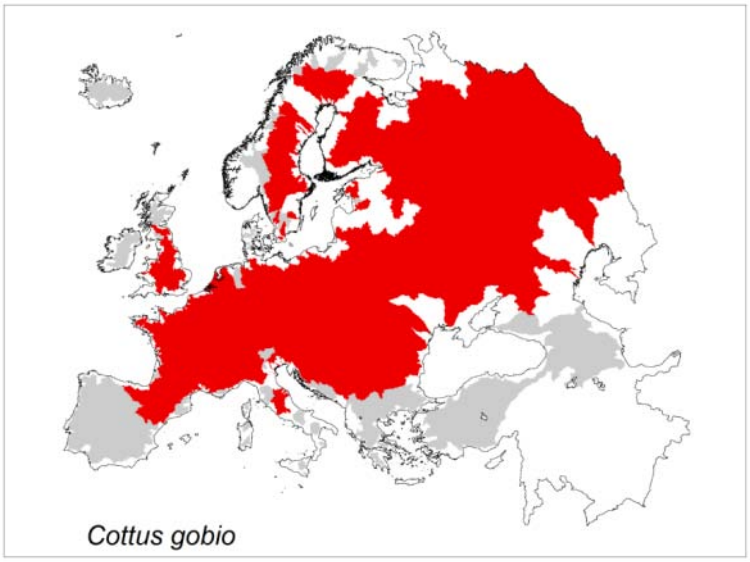
Cottus gobio

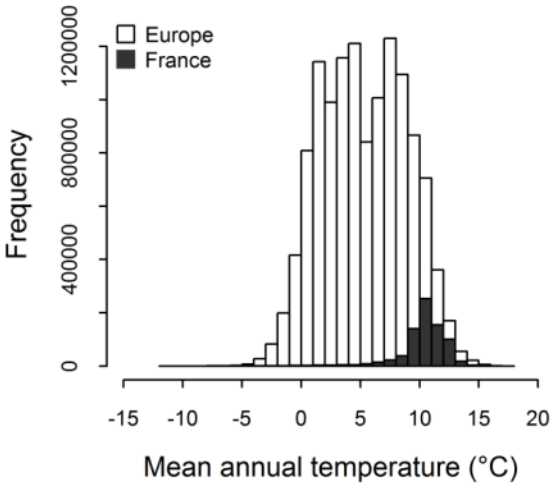
Europe
France
Frequency
0
400000
800000
1200000
-15
-10
-5
0
5
10
15
20
Mean annual temperature (°C)

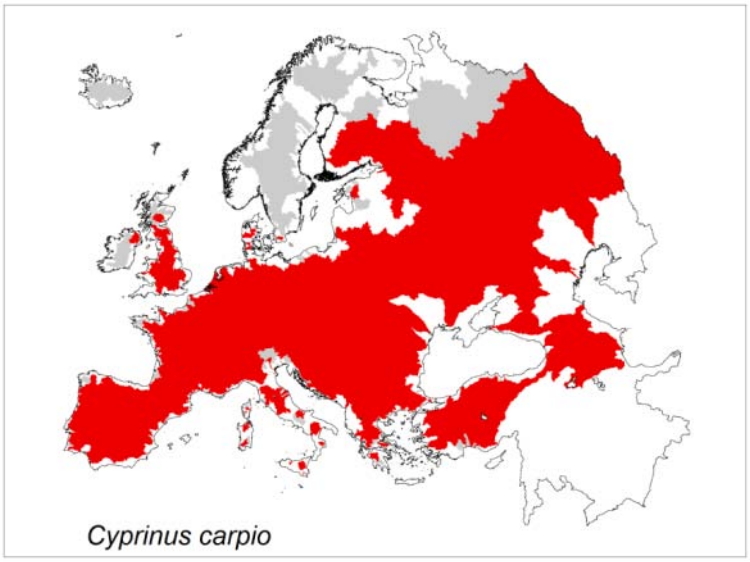
Cyprinus carpio

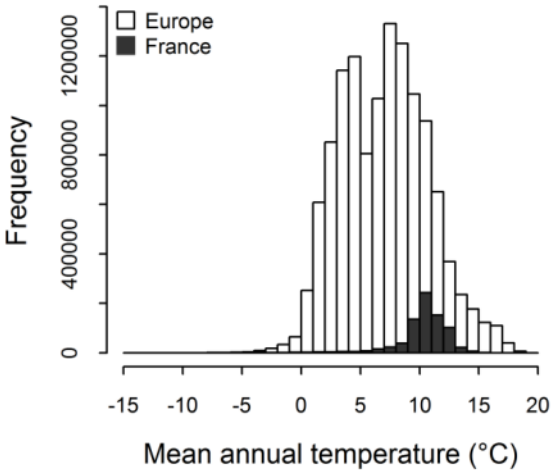
Europe
France
Frequency
0
400000
800000
1200000
-15
-10
-5
0
5
10
15
20
Mean annual temperature (°C)

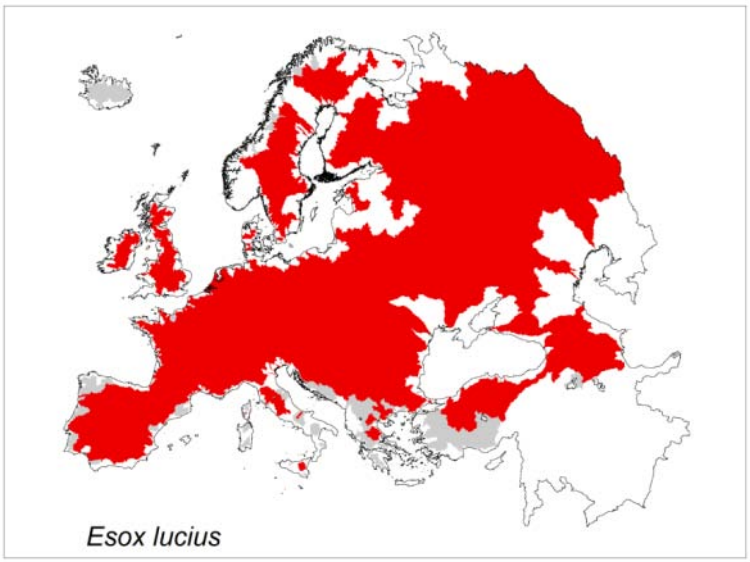

*Esox lucius*

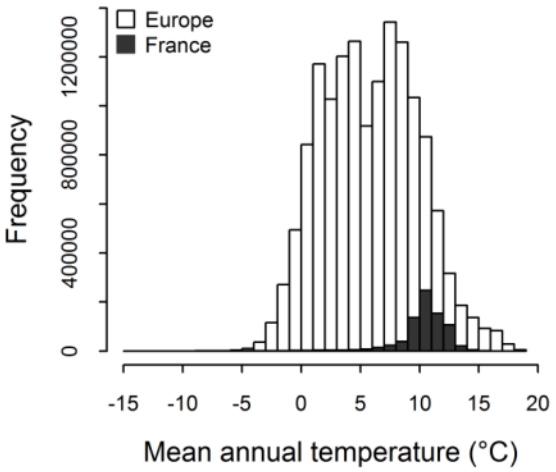


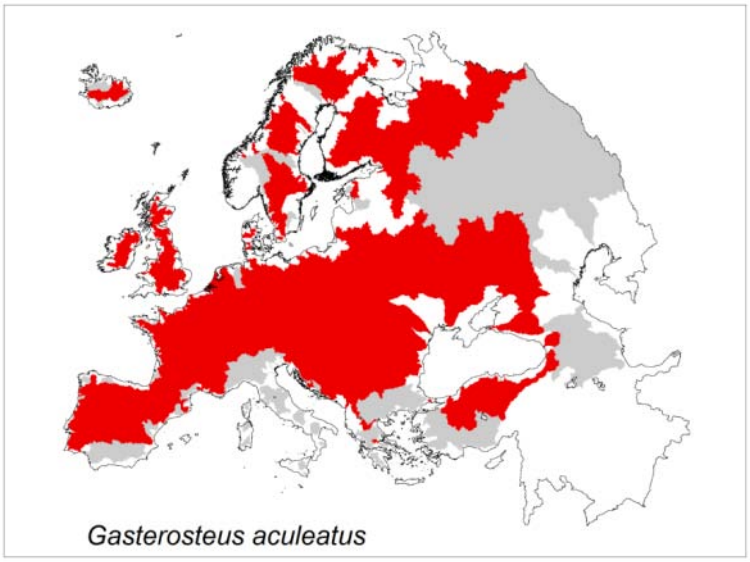

*Gasterosteus aculeatus*

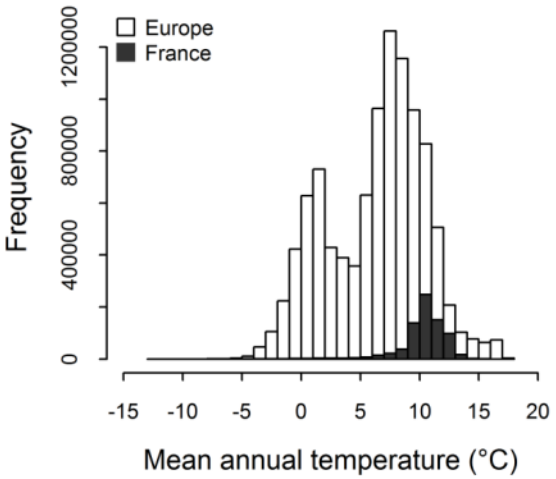


*Gobio gobio*

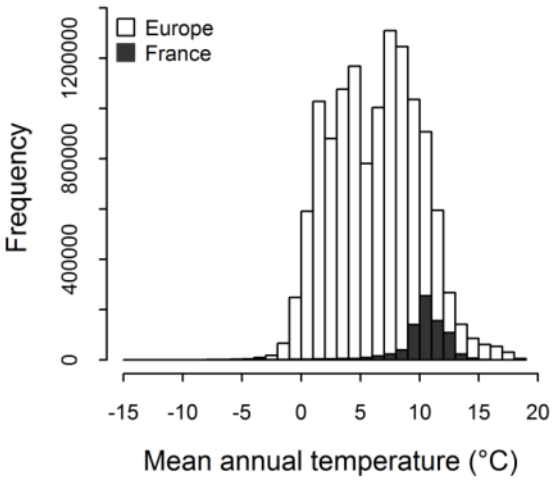

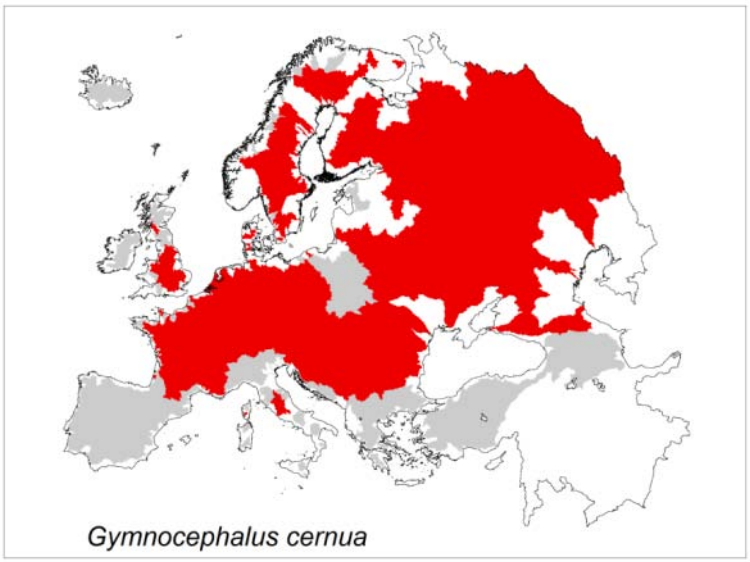

*Gymnocephalus cernua*

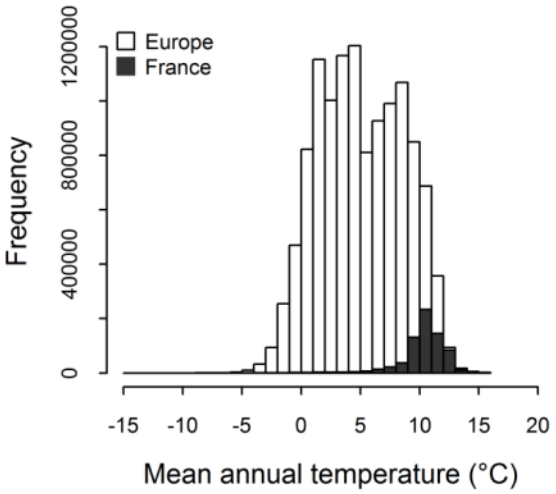


*Lepomis gibbosus*

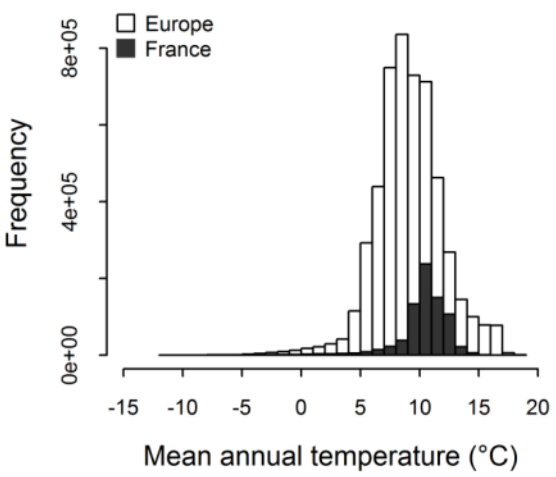


*Leuciscus leuciscus*

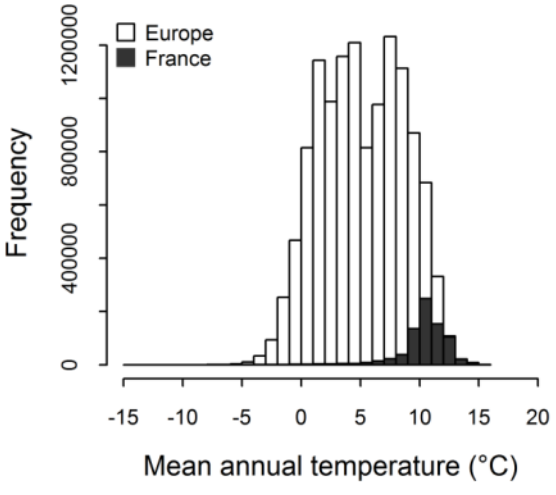


Lota lota

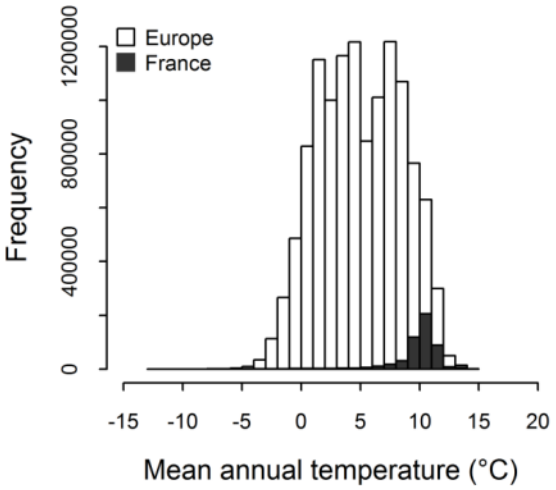
Europe
France
Frequency
0
400000
800000
1200000
-15
-10
-5
0
5
10
15
20
Mean annual temperature (°C)


Parachondrostoma toxostoma

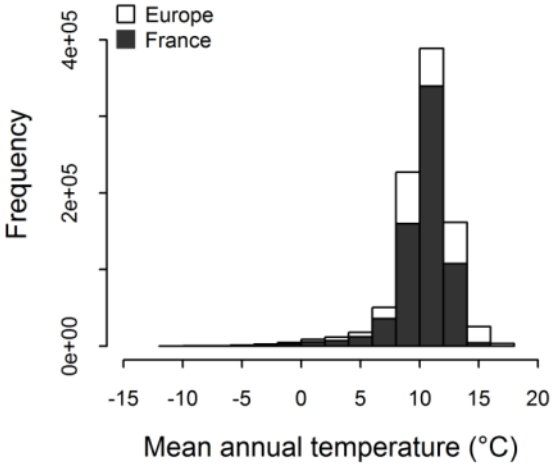
Europe
France
Frequency
0e+00
2e+05
4e+05
-15
-10
-5
0
5
10
15
20
Mean annual temperature (°C)

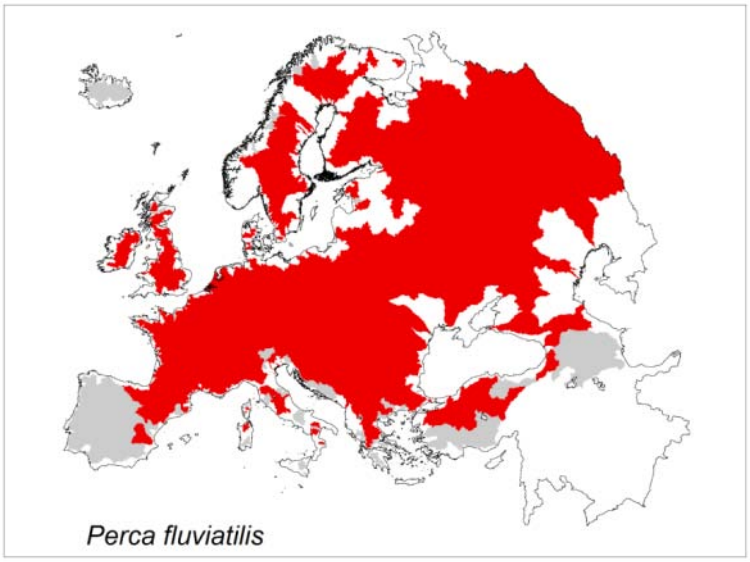
Perca fluviatilis

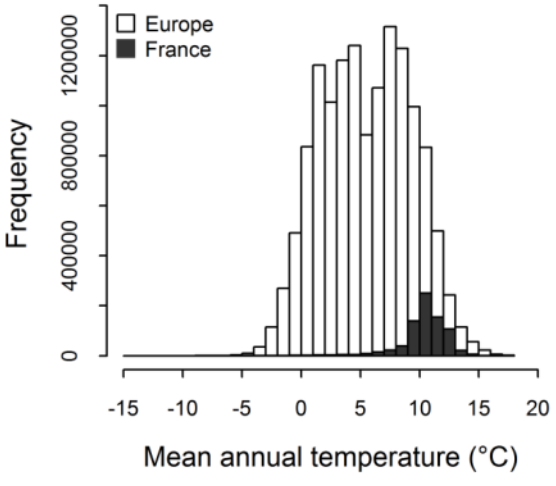
Europe
France
Frequency
0
400000
800000
1200000
-15
-10
-5
0
5
10
15
20
Mean annual temperature (°C)

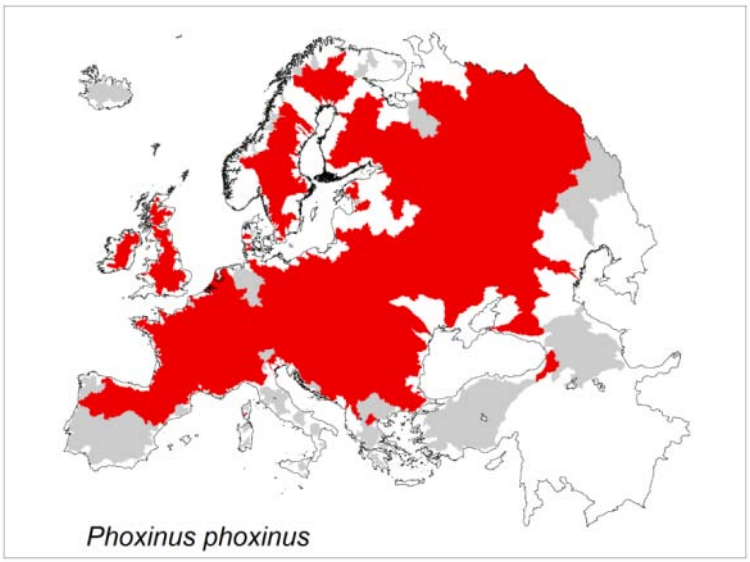
Phoxinus phoxinus

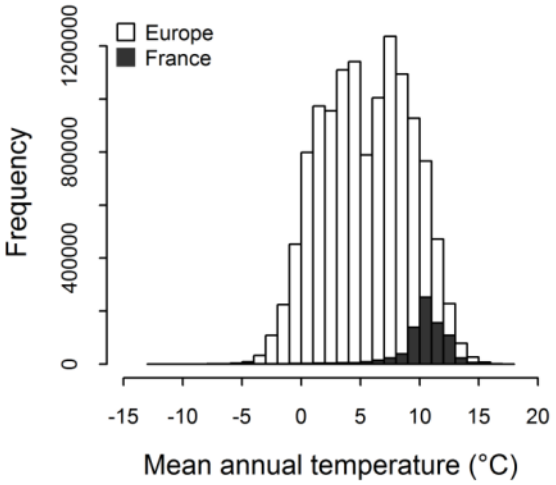
Europe
France
Frequency
0
400000
800000
1200000
-15
-10
-5
0
5
10
15
20
Mean annual temperature (°C)

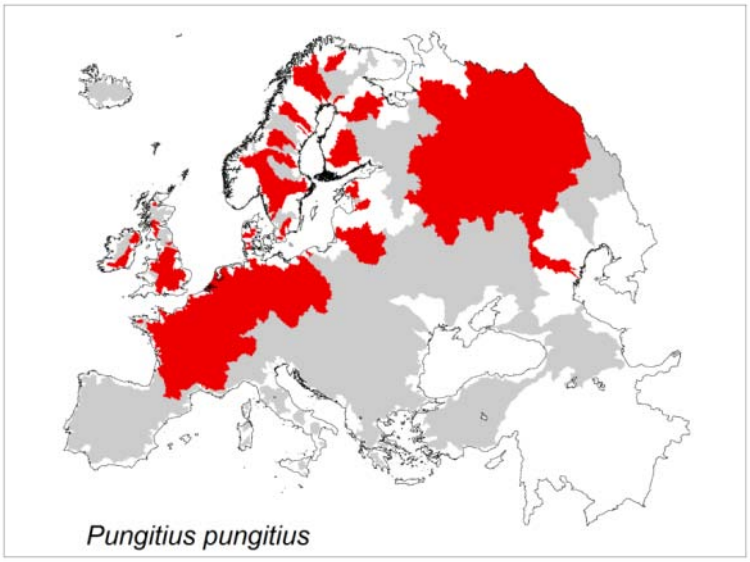
Pungitius pungitius

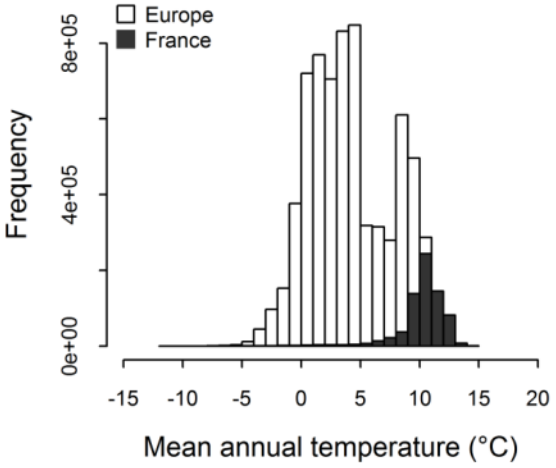
Europe
France
Frequency
0e+00
4e+05
8e+05
-15
-10
-5
0
5
10
15
20
Mean annual temperature (°C)

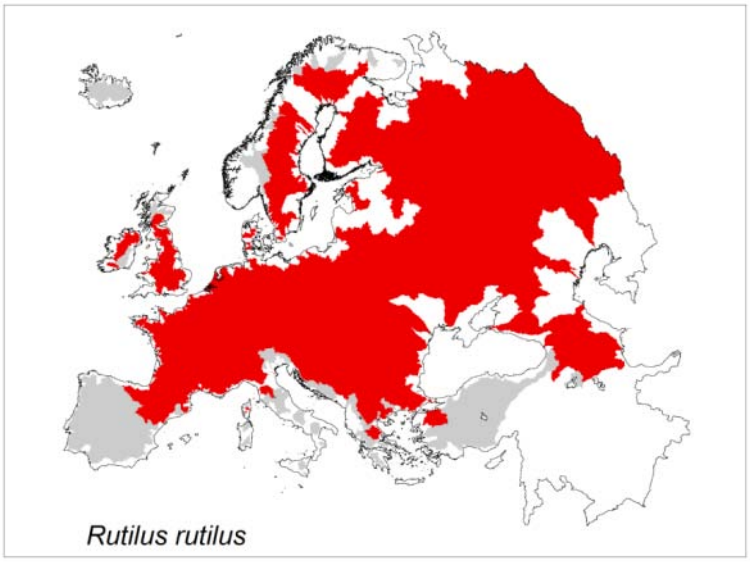
Rutilus rutilus

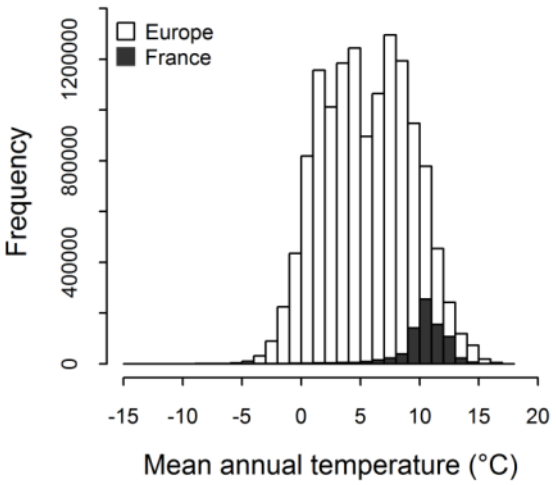
Europe
France
Frequency
0
400000
800000
1200000
-15
-10
-5
0
5
10
15
20
Mean annual temperature (°C)

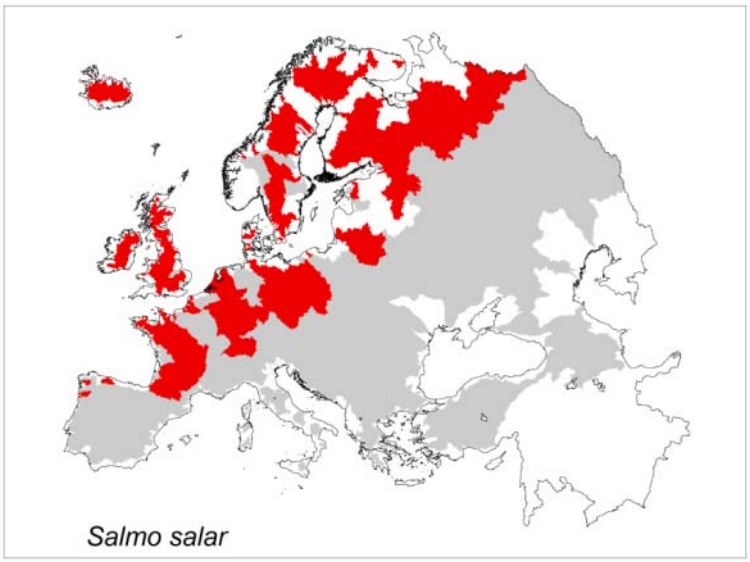
Salmo salar

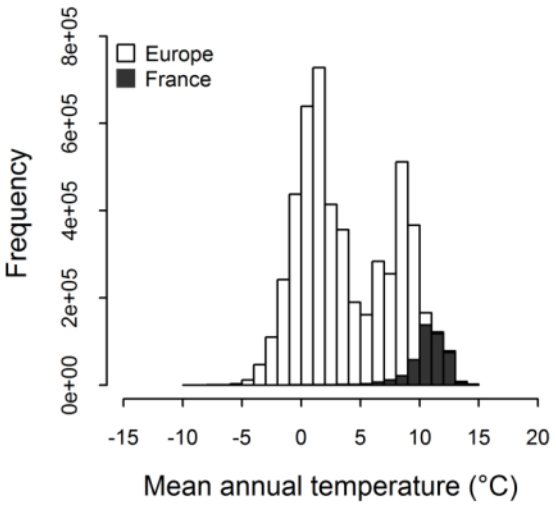
Europe
France
Frequency
0e+00
2e+05
4e+05
6e+05
8e+05
-15
-10
-5
0
5
10
15
20
Mean annual temperature (°C)

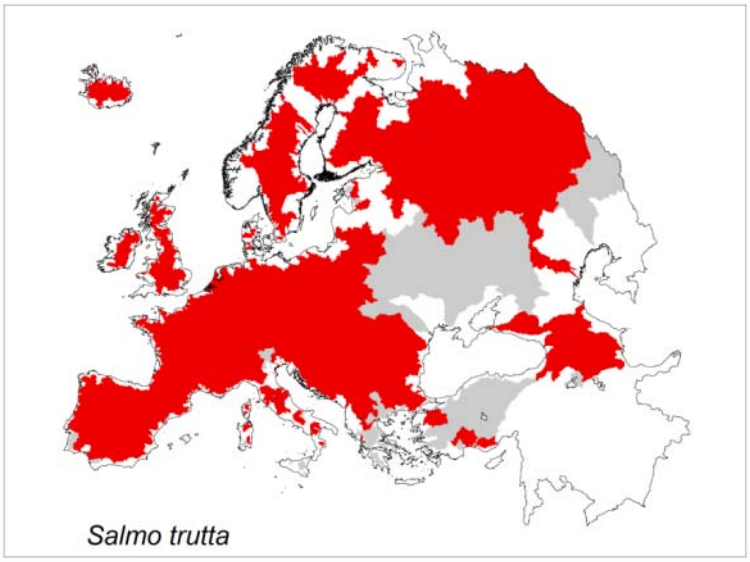
Salmo trutta

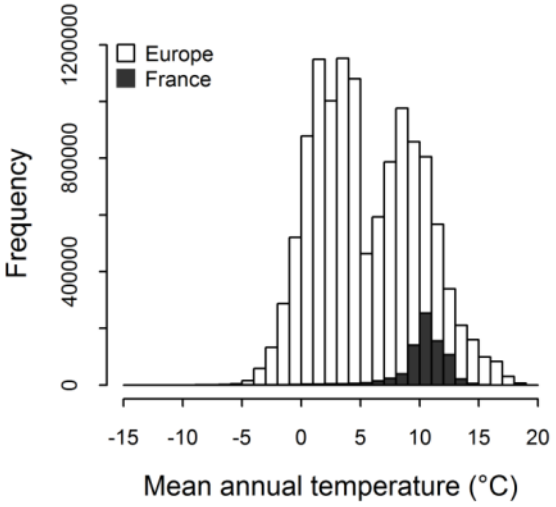
Europe
France
Frequency
0
400000
800000
1200000
-15
-10
-5
0
5
10
15
20
Mean annual temperature (°C)

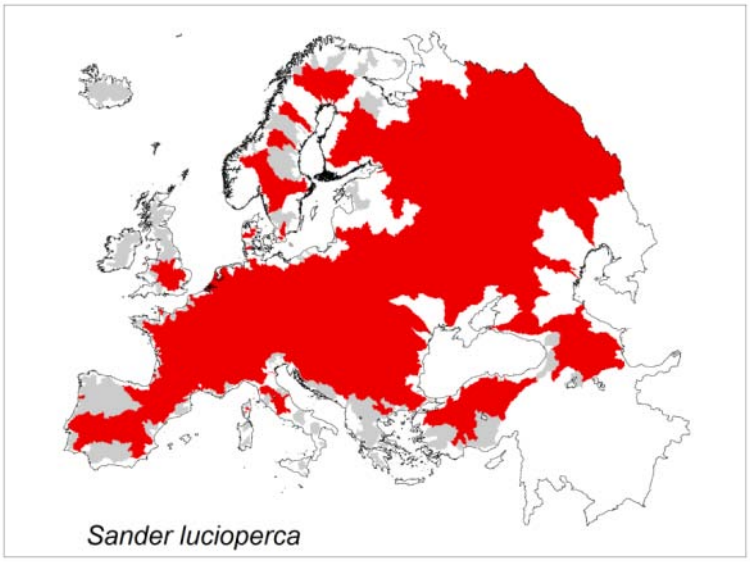
Sander lucioperca

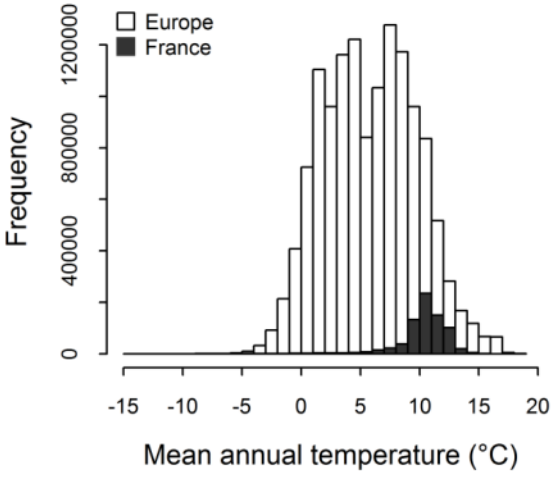
Europe
France
Frequency
0
400000
800000
1200000
-15
-10
-5
0
5
10
15
20
Mean annual temperature (°C)

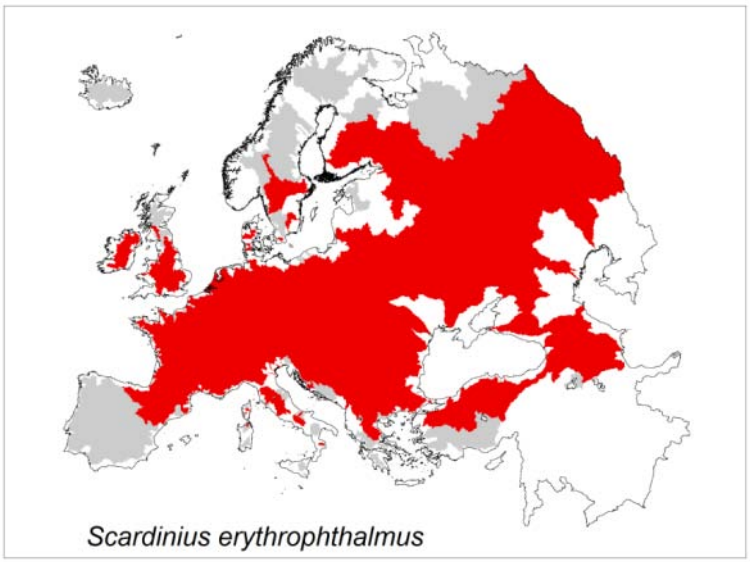
Scardinius erythrophthalmus

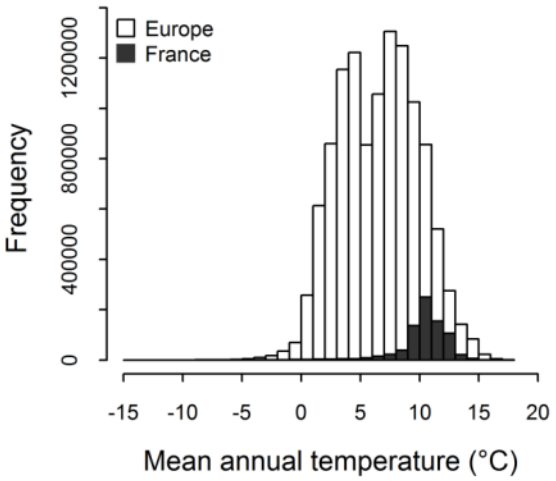
Europe
France
Frequency
0
400000
800000
1200000
-15
-10
-5
0
5
10
15
20
Mean annual temperature (°C)


Squalius cephalus

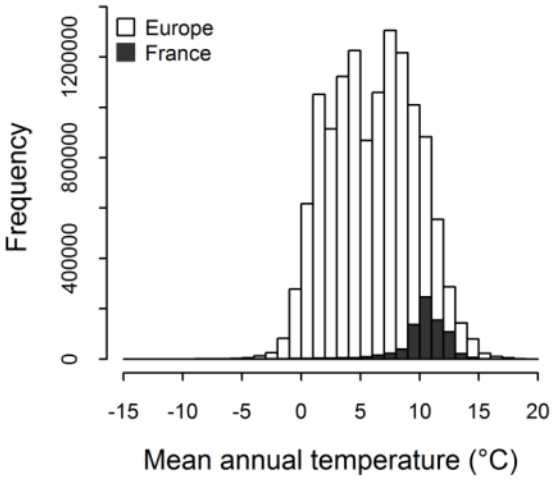
Europe
France
Frequency
0
400000
800000
1200000
-15
-10
-5
0
5
10
15
20
Mean annual temperature (°C)


Telestes souffia

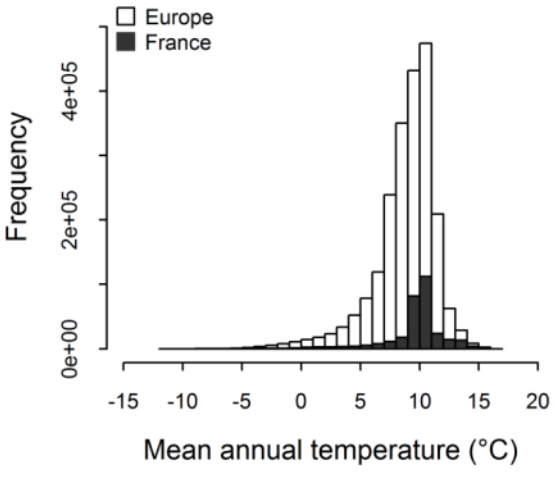
Europe
France
Frequency
0e+00
2e+05
4e+05
-15
-10
-5
0
5
10
15
20
Mean annual temperature (°C)

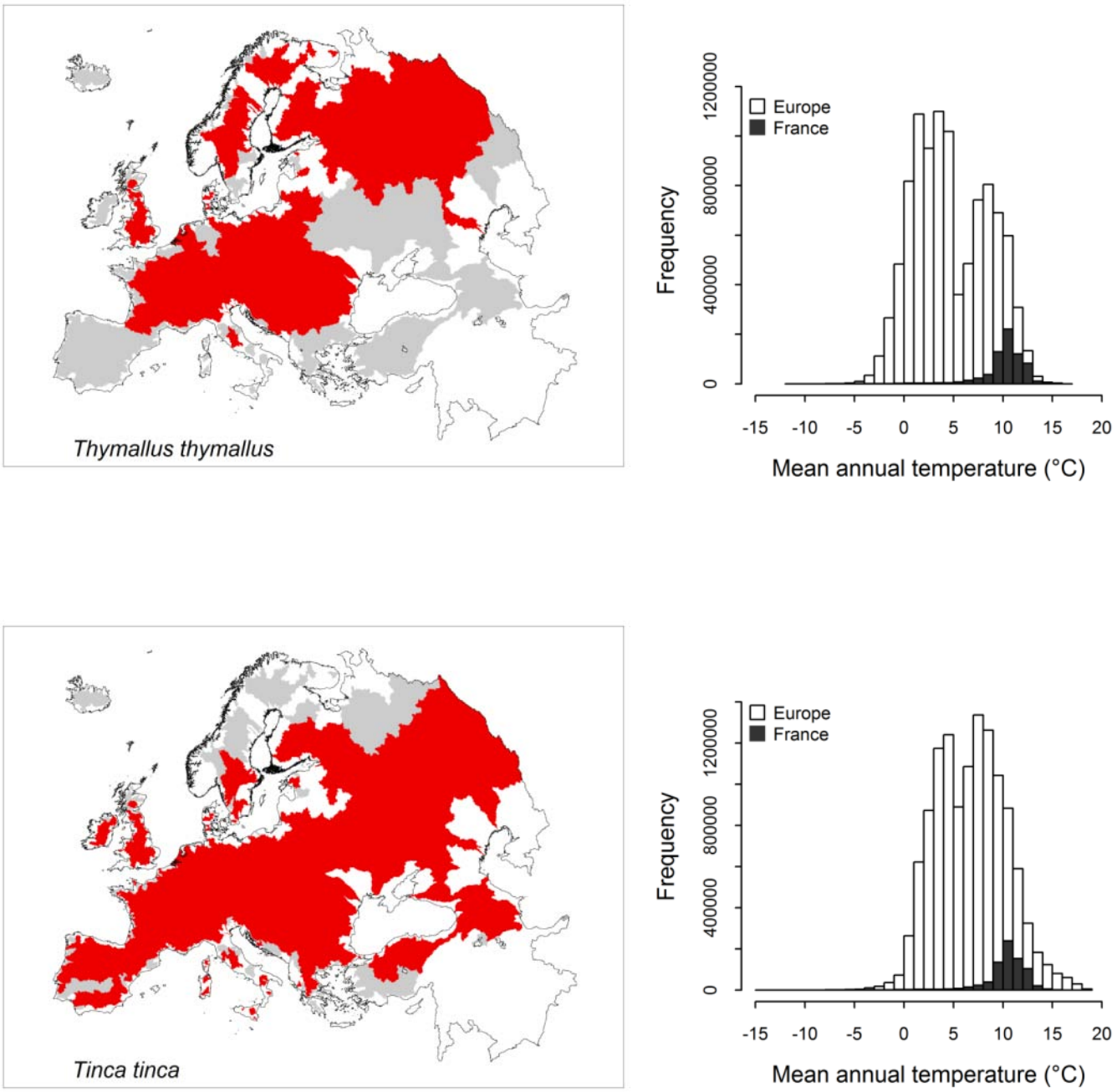


**Supplementary Figure 5 | Comparison of the climatic conditions across the European and French distributions of the studied species.** Spatial distributions of the 32 studied species across the 329 European catchments[3]: red for presence, grey for absence and white for unknown status[4], and histograms of the mean annual surface temperature encountered throughout the European (white) and the French (black) spatial distributions according to a climatic grid at a resolution of 30 arc-s (Supplementary Fig. 4).

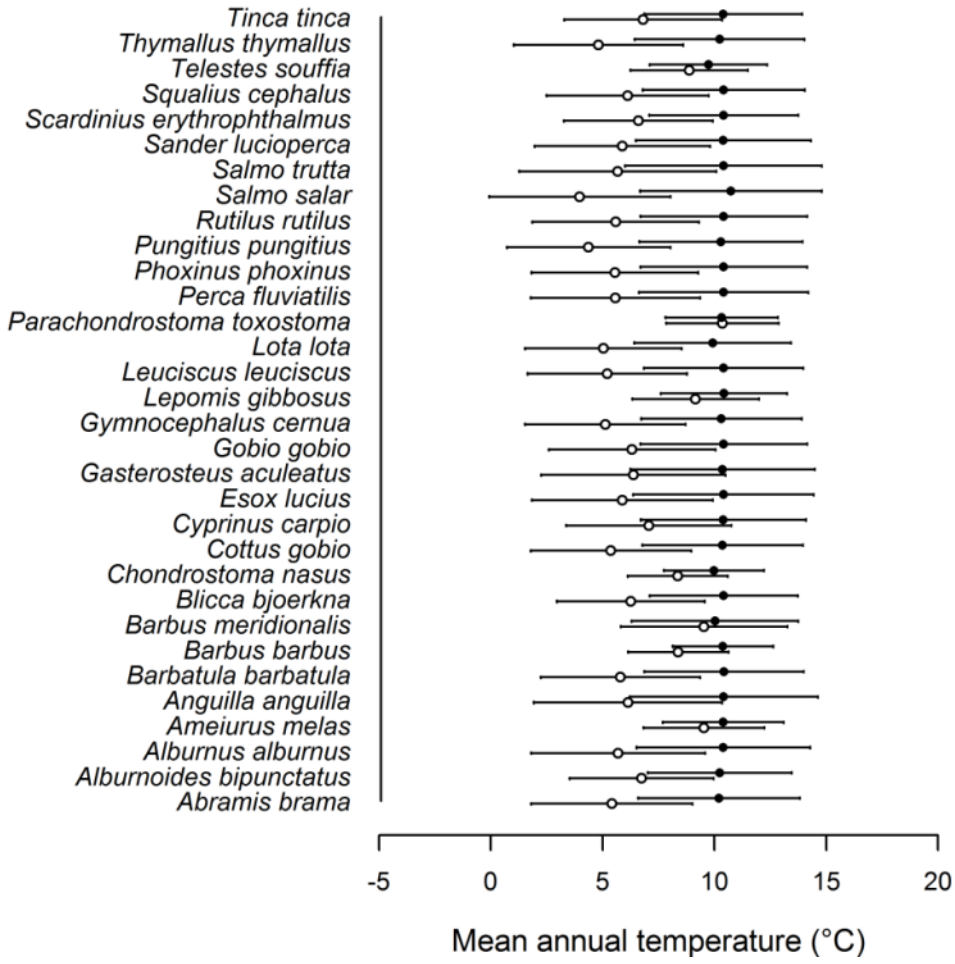


**Supplementary Figure 6 | Mean climatic conditions across the European and French distributions of the studied species.** Mean annual surface temperature (mean ± s.d., °C) encountered throughout the European (white) and the French (black) spatial distributions of the 32 studied species.

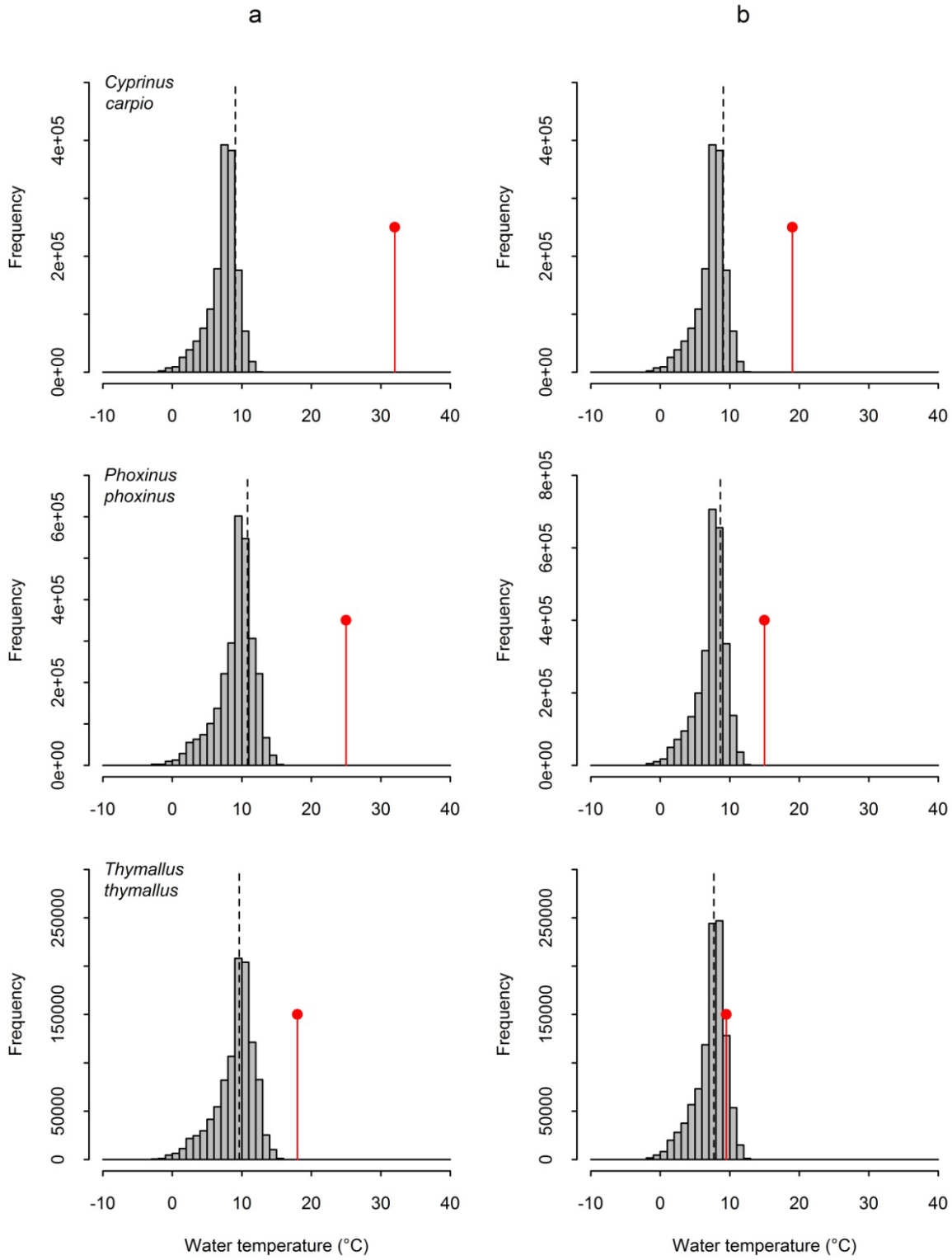


**Supplementary Figure 7 | Examples of the climatological temperature of three species habitats.** Mean annual water temperature across the French distribution in the initial period (grey histogram) for species with contrasted thermal preferences. The thermal safety margin[5] for each species is estimated through (**a**) $TSM_{opt}$: as the difference between the temperature of the species thermal habitat (dashed line: $T_{hab}$) and the upper limit of the optimal temperature range ($T_{opt}$: red dot) and (**b**) $TSM_{sp}$: as the difference between the temperature of the species thermal habitat (dashed line: $T_{hab}$) and the optimal spawning temperature ($T_{sp}$: red dot). $T_{hab}$ is calculated as the median value of the mean annual temperatures experienced by the species within the French hydrographic network and averaged across the 90 modelled spatial distributions.

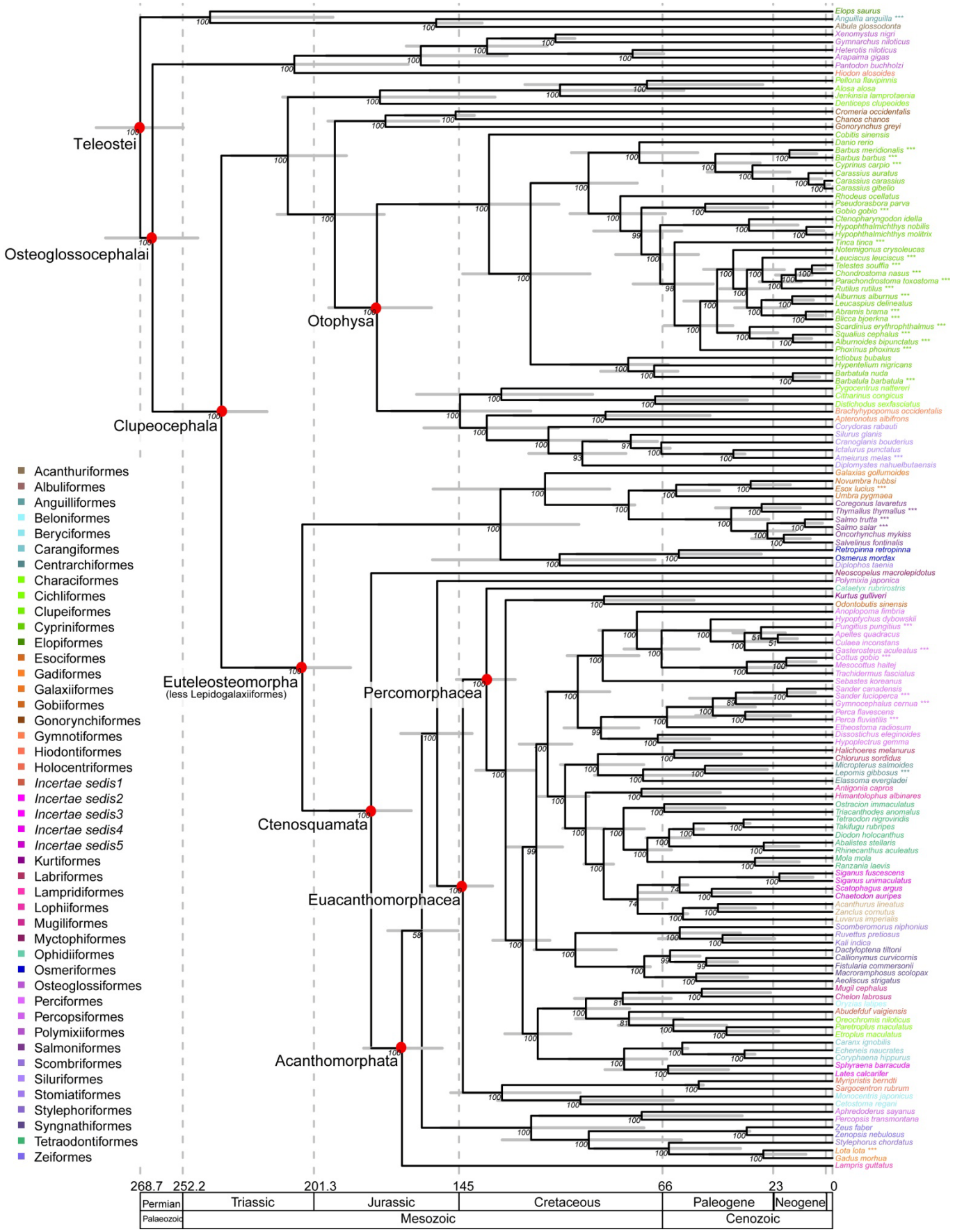


**Supplementary Figure 8 | Phylogenetic reconstruction.** Maximum clade credibility tree depicting the phylogenetic relationships of the 151 Teleostei fish species, with median and 95% highest posterior density of divergence times. Posterior probabilities are displayed for each internal node. Colours indicate taxonomic orders. The 32 species considered in this study are indicated by ***.

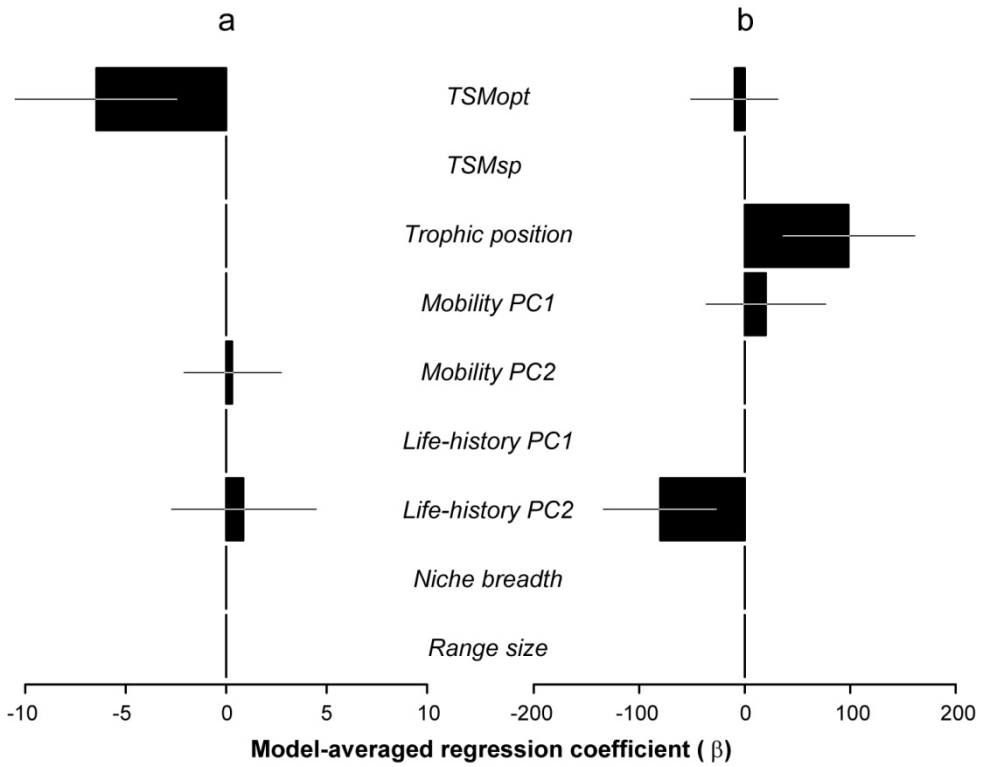


**Supplementary Figure 9 | Results of model averaging for models relating range shifts to species traits using the maximum clade credibility tree.** Model-averaged slope regression coefficients standardized to z-scores for PGLS relating shifts for 32 freshwater fish species at (**a**) the lower and (**b**) the upper altitudinal limit to species traits. Bars are 95% confidence interval. High values of m*obility PC1* and *mobility PC2* indicate a greater mobility at larval and adult stages, respectively. High values of *life-history PC1* and small values of *life-history PC2* indicate a greater propagule pressure.

**Supplementary Table 1 | Additional predictors.**

| Variable | Code | Description |
|---|---|---|
| Climate change velocity | *Velocity_up*<br>*Velocity_low* | Mean shift in mean annual temperature isotherms along the altitudinal gradient experienced by species at their upper or lower elevation limits in the initial period (m decade$^{-1}$)[1] |
| Popularity | *Popularity* | Number of results for the search of the Latin names of species in quotes using Google web browser restricted to French pages[6] |

Description of the variables used to control for the effects of potential extrinsic confounding factors.

**Supplementary Table 2 | Influence of additional predictors on the lower range shifts.**

| Source of variation | Deviance explained (%) | *F* | *p* |
|---|---|---|---|
| *Popularity* | 4.39 | 1.33 | 0.258 |
| *Velocity_low* | 0.13 | 0.04 | 0.844 |
| | Estimate (SE) | *t* | *p* |
| *Intercept* | 43.07 (192.62) | 0.22 | 0.825 |
| *Popularity* | -3.10 (2.71) | -1.15 | 0.262 |
| *Velocity_low* | -2.21 (0.91) | -0.20 | 0.844 |

Results of the generalized linear model linking the magnitude of shifts at the lower limit to the potential confounding factors.

**Supplementary Table 3 | Influence of additional predictors on the upper range shifts.**

| Source of variation | Deviance explained (%) | *F* | *p* | |
|---|---|---|---|---|
| *Popularity* | 0.54 | 0.22 | 0.643 | |
| *Velocity_up* | 28.56 | 11.68 | 0.002 | ** |
| | Estimate (SE) | *t* | *p* | |
| *Intercept* | -5794.37 (1729.64) | -3.35 | 0.002 | ** |
| *Popularity* | 21.84 (31.47) | 0.69 | 0.493 | |
| *Velocity_up* | 104.04 (30.44) | 3.42 | 0.002 | ** |

Results of the generalized linear model linking the rates of shifts at the upper limit to the potential confounding factors.

**Supplementary Table 4 | Description of species traits and modalities.**

| Trait | Code | Modality | Description |
|---|---|---|---|
| *Upper temperature limit* | $T_{opt}$ | - | Upper limit of the optimal temperature range (°C)[7, 8, 9] |
| *Spawning temperature* | $T_{sp}$ | - | Optimal spawning temperature (°C)[10] |
| *Trophic position* | TP | 1 | Herbivorous |
| | | 2 | Omnivorous |
| | | 3 | Invertivorous |
| | | 4 | Invertivorous-carnivorous |
| | | 5 | Piscivorous |
| *Body length* | BL | - | Total body length from the mouth to the fork of the tail (mm) |
| *Larval length* (at emergence) | LL | 1 | ≤ 4.2mm |
| | | 2 | 4.2-6.3mm |
| | | 3 | > 6.3mm |
| *Shape factor* | SH | - | Ratio of total body length to maximum body depth[11] |
| *Swimming factor* | SW | - | Ratio of the minimal depth of the caudal peduncle to maximum caudal fin depth[11] |
| *Range size* | range_size | | % of total network length in the initial period |
| *Niche breadth* | niche_breadth | - | Niche breadth on the first axis of the Outlying Mean Index (OMI[12]) based on 3 environmental variables: slope, elevation and upstream-downstream position |
| *Fecundity* (# oocytes) | FE | 1 | ≤ 10,000 |
| | | 2 | 10,000-100,000 |
| | | 3 | > 100,000 |
| *Egg diameter* (at hatching) | ED | 1 | < 1.35 mm |
| | | 2 | 1.35-2 mm |
| | | 3 | > 2 mm |
| *Life span* | LS | 1 | < 8 years |
| | | 2 | 8-15 years |
| | | 3 | > 15 years |
| *Female maturity* | MA | 1 | 1-2 years |
| | | 2 | 2-3 years |
| | | 3 | 3-4 years |
| | | 4 | 4-5 years |
| | | 5 | ≥ 5 years |
| *Parental care* | PC | 1 | No protection |
| | | 2 | No protection with nest or egg hiders |
| | | 3 | nest or egg hiders |
| *Incubation period* | IP | 1 | ≤ 7 days |
| | | 2 | 7-14 days |
| | | 3 | > 14 days |

**Supplementary Table 5 | Interpretation of synthetic traits.**

| | | Correlation | |
|---|---|---|---|
| | Trait | PC 1 | PC 2 |
| Mobility | | (31.7%) | (19.5%) |
| | *Body length* | -0.01 | 0.74 |
| | *Larval length* | 0.89 | 0.47 |
| | *Shape factor* | -0.56 | 0.44 |
| | *Swimming factor* | -0.22 | 0.37 |
| Life-history | | (26.7%) | (23.3%) |
| | *Fecundity* | 0.70 | -0.56 |
| | *Spawn time* | -0.47 | -0.84 |
| | *Egg diameter* | 0.07 | 0.55 |
| | *Life span* | 0.91 | 0.03 |
| | *Female maturity* | 0.84 | 0.14 |
| | *Incubation period* | -0.42 | 0.67 |
| | *Parental care* | -0.40 | 0.18 |

Correlations between species traits and the first two axes of the PCoA. Percentages in parentheses indicate the relative contribution of the axes to the PCoA.

**Supplementary Table 6 | Material used for the phylogenetic reconstruction.**

| Species | GenBank accession numbers | Order |
|---|---|---|
| *Abalistes stellaris* | NC_011943 | Tetraodontiformes |
| *Abramis brama* | AP009305 | Cypriniformes |
| *Abudefduf vaigiensis* | NC_009064 | *Incertae sedis* |
| *Acanthurus lineatus* | NC_010108 | Acanthuriformes |
| *Aeoliscus strigatus* | NC_010270 | Syngnathiformes |
| *Albula glossodonta* | NC_005800 | Albuliformes |
| *Alburnoides bipunctatus* | AJ247072 (*16S*); HQ960437 (*COX1*); HM560059 (*CytB*); Y12665 (*12S*) | Cypriniformes |
| *Alburnus alburnus* | AB239593 | Cypriniformes |
| *Alosa alosa* | AP009131 | Clupeiformes |
| *Ameiurus melas* | DQ421876 (*16S*); EU523906 (*COX1*); AY184273 (*CytB*); JN015532 (*12S*) | Siluriformes |
| *Anguilla anguilla* | AP007233 | Anguilliformes |
| *Anoplopoma fimbria* | NC_018119 | Perciformes |
| *Antigonia capros* | NC_003191 | Lophiiformes |
| *Apeltes quadracus* | NC_011580 | Perciformes |
| *Aphredoderus sayanus* | NC_004372 | Percopsiformes |
| *Apteronotus albifrons* | NC_004692 | Gymnotiformes |
| *Arapaima gigas* | NC_010570 | Osteoglossiformes |
| *Barbatula barbatula* | DQ077970 (*16S*); HQ960954 (*COX1*); DQ105254 (*CytB*) | Cypriniformes |
| *Barbatula nuda* | NC_022858 | Cypriniformes |
| *Barbus barbus* | AB238965 | Cypriniformes |
| *Barbus meridionalis* | AJ247061 (*16S*); JF798256 (*CytB*) | Cypriniformes |
| *Blicca bjoerkna* | AP009304 | Cypriniformes |
| *Brachyhypopomus occidentalis* | NC_015078 | Gymnotiformes |
| *Callionymus curvicornis* | NC_018567 | Syngnathiformes |
| *Caranx ignobilis* | NC_022932 | Carangiformes |
| *Carassius auratus* | AB006953 | Cypriniformes |
| *Carassius carassius* | JQ911695 | Cypriniformes |
| *Carassius gibelio* | GU170401 | Cypriniformes |
| *Cataetyx rubrirostris* | NC_004375 | Ophidiiformes |
| *Cetostoma regani* | NC_004389 | Beryciformes |
| *Chaetodon auripes* | NC_009870 | *Incertae sedis* |
| *Chanos chanos* | NC_004693 | Gonorynchiformes |
| *Chelon labrosus* | JF911706 | Mugiliformes |
| *Chlorurus sordidus* | NC_006355 | Labriformes |
| *Chondrostoma nasus* | DQ447691 (*16S*); HQ960429 (*COX1*); AF533760 (*CytB*); DQ455047 (*12S*) | Cypriniformes |
| *Citharinus congicus* | NC_015805 | Characiformes |
| *Cobitis sinensis* | NC_007229 | Cypriniformes |
| *Coregonus lavaretus* | AB034824 | Salmoniformes |
| *Corydoras rabauti* | NC_004698 | Siluriformes |
| *Coryphaena hippurus* | NC_023123 | Carangiformes |

| | | |
|---|---|---|
| *Cottus gobio* | HQ960512 (*COX1*); AY116366 (*CytB*); AB188189 (*12S*); HM050100 (*ND4*) | Perciformes |
| *Cranoglanis bouderius* | NC_008280 | Siluriformes |
| *Cromeria occidentalis* | NC_007881 | Gonorynchiformes |
| *Ctenopharyngodon idella* | JQ231115 | Cypriniformes |
| *Culaea inconstans* | NC_011577 | Perciformes |
| *Cyprinus carpio* | X61010 | Cypriniformes |
| *Dactyloptena tiltoni* | NC_004402 | Syngnathiformes |
| *Danio rerio* | NC_002333 | Cypriniformes |
| *Denticeps clupeoides* | NC_007889 | Clupeiformes |
| *Diodon holocanthus* | NC_009866 | Tetraodontiformes |
| *Diplomystes nahuelbutaensis* | NC_015823 | Siluriformes |
| *Diplophos taenia* | NC_002647 | Stomiatiformes |
| *Dissostichus eleginoides* | NC_018135 | Perciformes |
| *Distichodus sexfasciatus* | NC_015836 | Characiformes |
| *Echeneis naucrates* | NC_022508 | Carangiformes |
| *Elassoma evergladei* | NC_003175 | Centrarchiformes |
| *Elops saurus* | NC_005803 | Elopiformes |
| *Esox lucius* | AP004103 | Esociformes |
| *Etheostoma radiosum* | NC_005254 | Perciformes |
| *Etroplus maculatus* | NC_011179 | Cichliformes |
| *Fistularia commersonii* | NC_010274 | Syngnathiformes |
| *Gadus morhua* | NC_002081 | Gadiformes |
| *Galaxias gollumoides* | NC_015239 | Galaxiiformes |
| *Gasterosteus aculeatus* | NC_003174 | Perciformes |
| *Gobio gobio* | AB239596 | Cypriniformes |
| *Gonorynchus greyi* | NC_004702 | Gonorynchiformes |
| *Gymnarchus niloticus* | NC_012707 | Osteoglossiformes |
| *Gymnocephalus cernua* | AY141443 (*16S*); JN026731 (*COX1*); AF045356 (*CytB*); AY141373 (*12S*); JQ088605 (*ND2*); HM050108 (*ND4*) | Perciformes |
| *Halichoeres melanurus* | NC_009066 | Labriformes |
| *Heterotis niloticus* | NC_015081 | Osteoglossiformes |
| *Himantolophus albinares* | NC_013867 | Lophiiformes |
| *Hiodon alosoides* | NC_005145 | Hiodontiformes |
| *Hypentelium nigricans* | NC_008676 | Cypriniformes |
| *Hypophthalmichthys molitrix* | EU315941 | Cypriniformes |
| *Hypophthalmichthys nobilis* | EU343733 | Cypriniformes |
| *Hypoplectrus gemma* | NC_013832 | Perciformes |
| *Hypoptychus dybowskii* | NC_004400 | Perciformes |
| *Ictalurus punctatus* | NC_003489 | Siluriformes |
| *Ictiobus bubalus* | NC_013071 | Cypriniformes |
| *Jenkinsia lamprotaenia* | NC_006917 | Clupeiformes |
| *Kali indica* | NC_022488 | Scombriformes |
| *Kurtus gulliveri* | NC_022477 | Kurtiformes |
| *Lampris guttatus* | NC_003165 | Lampridiformes |
| *Lates calcarifer* | NC_007439 | *Incertae sedis* |

| | | |
|---|---|---|
| *Lepomis gibbosus* | AY742524 (*16S*); HQ557271 (*COX1*); JF742829 (*CytB*); JN655528 (*12S*); AB271766 (*ND1*); AY517735 (*ND2*) | Centrarchiformes |
| *Leucaspius delineatus* | AP009307 | Cypriniformes |
| *Leuciscus leuciscus* | GQ406268 (*16S*); HQ960728 (*COX1*); AY509823 (*CytB*) | Cypriniformes |
| *Lota lota* | AP004412 | Gadiformes |
| *Luvarus imperialis* | NC_009851 | Acanthuriformes |
| *Macroramphosus scolopax* | NC_010265 | Syngnathiformes |
| *Mesocottus haitej* | NC_022181 | Perciformes |
| *Micropterus salmoides* | DQ536425 | Centrarchiformes |
| *Mola mola* | NC_005836 | Tetraodontiformes |
| *Monocentris japonicus* | NC_004392 | Beryciformes |
| *Mugil cephalus* | AP002930 | Mugiliformes |
| *Myripristis berndti* | NC_003189 | Holocentriformes |
| *Neoscopelus macrolepidotus* | NC_020150 | Myctophiformes |
| *Notemigonus crysoleucas* | NC_008646 | Cypriniformes |
| *Novumbra hubbsi* | NC_022455 | Esociformes |
| *Odontobutis sinensis* | NC_022818 | Gobiiformes |
| *Oncorhynchus mykiss* | DQ288269 | Salmoniformes |
| *Oreochromis niloticus* | NC_013663 | Cichliformes |
| *Oryzias latipes* | NC_004387 | Beloniformes |
| *Osmerus mordax* | NC_015246 | Osmeriformes |
| *Ostracion immaculatus* | NC_009865 | Tetraodontiformes |
| *Pantodon buchholzi* | NC_003096 | Osteoglossiformes |
| *Parachondrostoma toxostoma* | AJ247040 (*16S*); AF533758 (*CytB*) | Cypriniformes |
| *Paretroplus maculatus* | NC_011177 | Cichliformes |
| *Pellona flavipinnis* | NC_014268 | Clupeiformes |
| *Perca flavescens* | NC_019572 | Perciformes |
| *Perca fluviatilis* | JQ999985 (*16S*); HQ600749 (*COX1*); AF045358 (*CytB*); JQ999988 (*12S*); JQ088607 (*ND2*); HM050129 (*ND4*) | Perciformes |
| *Percopsis transmontana* | NC_003168 | Percopsiformes |
| *Phoxinus phoxinus* | AP009309 | Cypriniformes |
| *Polymixia japonica* | NC_002648 | Polymixiiformes |
| *Pseudorasbora parva* | JF802126 | Cypriniformes |
| *Pungitius pungitius* | AB445130 | Perciformes |
| *Pygocentrus nattereri* | NC_015840 | Characiformes |
| *Ranzania laevis* | NC_007887 | Tetraodontiformes |
| *Retropinna retropinna* | NC_004598 | Osmeriformes |
| *Rhinecanthus aculeatus* | NC_011941 | Tetraodontiformes |
| *Rhodeus ocellatus* | NC_011211 | Cypriniformes |
| *Rutilus rutilus* | GQ406271 (*16S*); HQ960426 (*COX1*); HM156759 (*CytB*); AF038484 (*12S*); HM209401 (*COX2*) | Cypriniformes |
| *Ruvettus pretiosus* | NC_022493 | Scombriformes |
| *Salmo salar* | U12143 | Salmoniformes |
| *Salmo trutta* | JQ390057 | Salmoniformes |
| *Salvelinus fontinalis* | AF154850 | Salmoniformes |

| | | |
|---|---|---|
| *Sander canadensis* | NC_021444 | Perciformes |
| *Sander lucioperca* | JQ999986 (*16S*); JQ623977 (*COX1*); JX025365 (*CytB*); JQ999990 (*12S*); JQ088643 (*ND2*); HM050136 (*ND4*) | Perciformes |
| *Sargocentron rubrum* | NC_004395 | Holocentriformes |
| *Scardinius erythrophthalmus* | AF215479 (*16S*); JQ623983 (*COX1*); AY509836 (*CytB*); Y12668 (*12S*); EF112529 (*COX2*) | Cypriniformes |
| *Scatophagus argus* | NC_021968 | Incertae sedis |
| *Scomberomorus niphonius* | NC_016420 | Scombriformes |
| *Sebastes koreanus* | NC_023265 | Perciformes |
| *Siganus fuscescens* | NC_009572 | *Incertae sedis* |
| *Siganus unimaculatus* | NC_013148 | *Incertae sedis* |
| *Silurus glanis* | AM398435 | Siluriformes |
| *Sphyraena barracuda* | NC_022484 | *Incertae sedis* |
| *Squalius cephalus* | AJ247054 (*16S*); HQ960688 (*COX1*); Y10446 (*CytB*); Y12667 (*12S*) | Cypriniformes |
| *Stylephorus chordatus* | NC_009948 | Stylephoriformes |
| *Takifugu rubripes* | NC_004299 | Tetraodontiformes |
| *Telestes souffia* | DQ447688 (*16S*); HM560372 (*COX1*); AY509861 (*CytB*); DQ447663 (*12S*) | Cypriniformes |
| *Tetraodon nigroviridis* | NC_007176 | Tetraodontiformes |
| *Thymallus thymallus* | FJ853655 | Salmoniformes |
| *Tinca tinca* | AB218686 | Cypriniformes |
| *Trachidermus fasciatus* | NC_018770 | Perciformes |
| *Triacanthodes anomalus* | NC_009861 | Tetraodontiformes |
| *Umbra pygmaea* | AP013049 | Esociformes |
| *Xenomystus nigri* | NC_012715 | Osteoglossiformes |
| *Zanclus cornutus* | NC_009852 | Acanthuriformes |
| *Zenopsis nebulosus* | NC_003173 | Zeiformes |
| *Zeus faber* | NC_003190 | Zeiformes |

Species and sequences used to reconstruct the phylogenetic hypothesis of the 151 Teleostei fish considered in this study.

**Supplementary Table 7 | Calibration and prior settings used for divergence time estimates[13].**

| | Distribution type | 95% Hard min. age | 95% Soft max. age | Priors settings |
|---|---|---|---|---|
| Elopomorpha | uniform | 149 | 260 | |
| Albuliformes+Anguilliformes | exponential | 136 | 216 | mean = 27.70 |
| Osteoglossomorpha | uniform | 130 | 260 | |
| Notopteridae | exponential | 100 | 216 | mean = 28.73 |
| Arapaimidae | exponential | 65,5 | 136 | mean = 23.55 |
| Chanidae | exponential | 65,5 | 136 | mean = 25.70 |
| Cobitoidea | exponential | 60 | 146,5 | mean = 27.20 |
| Cyprinidae | exponential | 48,5 | 146,5 | mean = 27.20 |
| Ictaluridae+Cranoglanidae | exponential | 63 | 146,5 | mean = 27.87 |
| Ictaluridae | exponential | 34 | 63 | mean = 10.01 |
| Esocidae + Umbridae | lognormal | 76,5 | 87,5 | mean = 1.62; s.d. = 0.8 |
| Salmonidae | lognormal | 51,8 | 76,4 | mean = 1.62; s.d. = 0.8 |
| Percopsidae | lognormal | 51,8 | 76,4 | mean = 0.53; s.d. = 0.8 |
| Zenopsis+Zeus | lognormal | 32 | 36,5 | mean = 0.23; s.d. = 0.8 |
| Holocentridae | lognormal | 50 | 57,5 | mean = 0.67; s.d. = 0.8 |
| Syngnathiformes | lognormal | 70,5 | 81 | mean = 1.02; s.d. = 0.8 |
| Centriscidae | lognormal | 50 | 57,5 | mean = 0.67; s.d. = 0.8 |
| Carangiformes | lognormal | 56 | 64 | mean = 0.78; s.d. = 0.8 |
| Echeneidae+Coryphaenidae+ Rachycentridae | lognormal | 30 | 34,5 | mean = 0.17; s.d. = 0.8 |
| Luvaridae | lognormal | 56 | 64 | mean = 0.78; s.d. = 0.8 |
| Siganidae | lognormal | 56 | 64 | mean = 0.78; s.d. = 0.8 |
| Tetraodontiformes | exponential | 85 | 122 | mean = 11.69 |
| Tetraodontidae | exponential | 32 | 50 | mean = 6.01 |
| Diodontidae+Tetraodontidae | exponential | 50 | 85 | mean = 11.52 |
| Molidae | exponential | 41 | 85 | mean = 14.52 |
| Balistidae | exponential | 35 | 85 | mean = 16.52 |
| Teleostei | normal | 255 | 312 | mean = 283; s.d. = 18.0 |
| Osteoglossocephalai | normal | 245 | 302 | mean = 273; s.d. = 18.0 |
| Clupeocephala | normal | 225 | 276 | mean = 251; s.d. = 15.0 |
| Otophysa | normal | 176 | 225 | mean = 197; s.d. = 17.0 |
| Euteleosteomorpha (less Lepidogalaxiiformes) | normal | 185 | 233 | mean = 211; s.d. = 14.0 |
| Ctenosquamata | normal | 157 | 195 | mean = 273; s.d. = 14.0 |
| Acanthomorphata | normal | 146 | 188 | mean = 164; s.d. = 14.0 |
| Euacanthomorphacea | normal | 130 | 168 | mean = 145; s.d. = 14.0 |
| Percomorphacea | normal | 118 | 156 | mean = 133; s.d. = 14.0 |

**Supplementary Table 8 | Results of model selection for models relating range shifts to species traits using the maximum clade credibility tree.**

| | Model selection | | | | | |
|---|---|---|---|---|---|---|
| | Lower limit | | | Upper limit | | |
| Trait | M1 | M2 | M3 | M1 | M2 | M3 |
| *TSMopt* | ●* | ●** | ●** | | | ● |
| *TSMsp* | | | | | | |
| *Trophic position* | | | | ●* | ●* | ●* |
| *Mobility PC1* | | | | ● | | |
| *Mobility PC2* | | | ● | | | |
| *Life-history PC1* | | | | | | |
| *Life-history PC2* | | ● | | ●* | ●* | ●** |
| *Niche breadth* | | | | | | |
| *Range size* | | | | | | |
| *wi* | 0.45 | 0.33 | 0.22 | 0.5 | 0.29 | 0.26 |
| $R^2$ | 0.20 | 0.25 | 0.23 | 0.37 | 0.35 | 0.37 |

Model selection (M1 - M3) for PGLS built to investigate the relationships between shifts in the lower and upper altitudinal limits and species traits for 32 freshwater species. ● indicates a trait that was included in the model. $w_i$ is the model weight, and $R^2$ is calculated for each model as in eq. 2.3.16[14]. *$p$ < 0.05; **$p$ < 0.01; ***$p$ < 0.001

# Supplementary Methods

## 1. Species range shifts

**Study area and species.** Range shifts of freshwater fish were previously documented[1] based on the electrofishing database of the French National Agency for Water and Aquatic Environments (Onema), which provides a spatially and temporally extensive survey of freshwater fish at the national scale[10]. From this database, two well-balanced pools of sites were selected (Supplementary Fig. 1), sampled during "cold" and "warm" temperature regime periods. The first period included 3549 sites sampled from 1980 to 1992. The second period included 3543 sites sampled from 2003 to 2009. Data on the presence-absence of fish species were recorded at each site from 1 to 19 times during the initial period, and from 1 to 14 times during the contemporary period, resulting in 4533 and 7548 sampling records, respectively. After correcting for taxonomic revisions that had occurred during the entire study period (i.e. pooling together existing species in the initial period that have been divided into two or more species in the contemporary period), only species present on at least 75 sites in both periods were considered for analyses, for a total of 32 species.

**Climatic data.** To describe the thermal habitat of species, mean annual temperatures (°C) were extracted for each period and each reach of the French hydrographic network (CCM2[3]). Climatic variables were derived from the high resolution (8 km grid-data) SAFRAN atmospheric reanalysis over France[15]. Water temperature was obtained by applying a scaling factor of 0.8 to the surface temperature[16]. For both periods, the mean annual temperature was obtained by averaging the climatic variables within each period plus the three preceding years, which correspond to the mean duration of the species life cycle.

Temporal changes in mean annual water temperature indicated that the area studied had become warmer with an increase by about 0.55°C, although changes were not homogeneous across the hydrological network: higher altitudinal sites had warmed less than lower elevation sites ($p < 0.001$, $n = 100{,}888$; Supplementary Fig. 1).

**Modelling species distribution.** The occurrence of each species was modelled independently for both time periods as a function of several topographic and climatic variables (Supplementary Fig. 2). Datasets for each period were composed of one sampling record (i.e. presence or absence) randomly chosen for each site, to avoid pseudoreplication. To take into account the variability introduced by the modelling method, a consensus approach was used by averaging the probabilities of occurrence predicted by eight single-SDMs[17]: generalised linear models, generalised additive models, multivariate adaptive regression splines, mixture discriminant analyses, classification and regression trees, random forest, generalised boosted trees and artificial neural networks. Models were calibrated on 70% of the sites, while the remaining 30% were used for evaluation and threshold selection (Supplementary Fig. 2, step 1). The calibrated models were then used to predict the probabilities of occurrence of the

species on the reaches of the French hydrographic network (scale: 2 km length) for which environmental conditions did not differ from those of the calibration datasets (Supplementary Fig. 2, step 2). These probabilities were then converted into binary predictions of presence and absence using three of the most common threshold-setting methods: threshold values maximising the sum of sensitivity and specificity, sensitivity equalling specificity and maximising Kappa. Finally, the different steps of the modelling process were repeated 30 times with 30 different datasets to take into account the variability due to the quality of the calibration dataset. At the end of the modelling process, 90 modelled species distributions were obtained for each period and species, resulting from 30 iterations and 3 thresholds. The different predictions were then aggregated to obtain a map describing the presence or absence of the species across the whole French hydrographic network while taking into account the uncertainty arising from different methodological choices (Supplementary Fig. 2, step 3).

**Estimating range descriptors.** The lower and upper range limits were defined for each modelled distribution as 2.5 and 97.5% of the altitudinal values of all predicted presences, respectively, in order to reduce the influence of outliers[18].

**Estimating range shifts.** As threshold selection is known to strongly influence species distribution modelling[19], temporal changes in range limits were evaluated by controlling for this effect. Multiple linear regression provides a way for adjusting for potentially confounding variables when assessing the effect of a predictor variable on a dependant variable[20]. To do so, linear regressions were fitted for each species between the measures of range limits (for either upper or lower altitudinal limit) estimated for the two time periods as a dependent variable ($\hat{Y}$) and the threshold-setting method (*Thresh*) and the period (*Period*) as explanatory factors (Supplementary Equation 1).

$$\hat{Y} = \beta 0 + \beta 1.Thresh + \beta 2.Period \qquad (1)$$

The shift (i.e. the magnitude of expansion or contraction) was then estimated by $\beta 2$, the regression coefficient of the period-group effect that quantifies the change in range limit in the contemporary period, adjusted for the threshold effect.

Contrasted changes were observed between species, and most of them shifted to higher elevation (Supplementary Fig. 3; lower: 4.85 m ± 14.92 s.d.; upper: 116.90 m ± 200.83 s.d.).

**Spatial distribution of the 32 species.** To ensure that we did not miss the response of species because we did not capture their entire spatial distribution, we compared the climatic conditions occurring throughout their European distribution and their French distribution (Supplementary Fig. 4; Supplementary Fig. 5). The climatic conditions found in France encompass the warm range limit for most of the studied species regarding the mean annual temperature. Although almost all of them have a pan-European distribution, the thermal

conditions they experience across France are among the warmest they experience across their whole European distribution and are in average warmer (Supplementary Fig. 6; *t*-test, $p < 0.001$ except for *P. toxotsoma* which is endemic to French hydrographic basins).

## 2. Phylogenetic reconstruction

**Molecular data.** A total of 151 Teleostei fish species were targeted for this study, including the 32 studied species as well as 119 other species, allowing to cover the major fish clades and for which divergence date estimates were available for phylogenetic reconstruction. The taxonomic sampling consists of 142 genera, 91 families, and 41 orders following the most updated taxonomy of Teleostei fish[13].

The complete mitochondrial genomes were examined for a total of 14 mitonchondrial genes: cytochrome b (*CytB*), cytochrome oxidase I (*COX1*), cytochrome oxidase II (*COX2*), cytochrome oxidase III (*COX3*), NADH dehydrogenase subunit 1 (*ND1*), 2 (*ND2*), 3 (*ND3*), 4 (*ND4*), 4L (*ND4L*) and 5 (*ND5*), *ATP6*, *ATP8* and ribosomal 12S (*12S*) and 16S (*16S*) sub-units. Sequences were obtained from GenBank®. A complete list of material examined is given in Supplementary Table 6.

**Sequence alignment and phylogenetic analyses.** For the ribosomal genes, molecular sequences were aligned using Muscle 3.8.31_i86linux64[21] most accurate algorithm and no manual adjustment was performed. Randomly similar sections within the alignments were identified and removed using Aliscore.02.2[22]. A window size of 6 positions was used and gaps were treated as ambiguous characters. Ambiguous regions were further discarded using trimAl v1.4[23] with an automatic selection method based on similarity statistics (-automated1 option). The protein-coding sequences were aligned using translatorX[24] to ensure conservation of the reading frame. Because of the old age of the group, data saturation is a serious concern that needs to be carefully addressed. For the coding gene, we evaluated the saturation of the full dataset, 1st and 2nd codon positions together and finally 3rd codon positions. Following[25], we estimated saturation in the R package *ape* 3.0-8[26] by calculating the slope of the scatterplot of uncorrected versus K80 corrected distances[27] of all taxon pairs. Removing the third codon position (slope = 0.18, 0.09, 0.12, 0.12, 0.06, 0.06, 0.03, 0.10, 0.06, 0.70, 0.11, 0.05 for *CytB*, *COX1*, *COX2*, *COX3*, *ND1*, *ND3*, *ND4*, *ND4L*, *ND5*, and *ATP6*, respectively) allows to discard most of the saturation in this dataset (slope = 0.86, 0.93, 0.86, 0.9, 0.81, 0.78, 0.8, 0.79, 0.79, 0.77, 0.79). However, due to the high level of saturation of *ATP8* and *ND2* even after excluding the third codon position (slope = 0.58, 0.73), these genes were excluded from the final partition. The best partitioning scheme was estimated using a heuristic approach implemented in PartitionFinder[28]. The best partition scheme was found to be: (*ATP6*, *ND3*, *ND4*) (*COX1*) (*COX2*, *COX3*) (*CytB*, *ND1*, *ND4L*) (*ND5*) (*12S*) (*16S*) and consisted of 9301 base pairs.

**Divergence time estimates.** Divergence times were estimated using a Bayesian approach with BEAST v1.8.0[29]. We implemented an uncorrelated log-normal (UCLN) clock-model with priors based on previous estimates of molecular rates of change[30]. To temporally calibrate the phylogenetic tree, we selected 26 geological calibration points as priors for divergence time estimates and we placed additional constraints on divergence times at five of the major nodes spread across the phylogeny from a previous published study[13] (Supplementary Table 7). To model branching rates on the tree, a birth-death process was used for the tree prior with initial birth rate = 1.0 and death rate = 0.5. Clock and tree priors were linked across partitions. Five replicates of the Markov chain Monte Carlo (MCMC) analyses were each run for 70 million generations, sampling trees and parameters values every 10,000 generations. The topology was constrained to that recovered in the phylogenetic estimates the monophyly of the main clades, orders and calibration points[13]. A chronogram that satisfied monophyly and initial divergence times of calibration points was used as a staring tree. After confirming convergence of the five runs using Tracer v1.6, we combined the post-burn-in samples of the five runs in LogCombiner v1.8.0 with the first 10% of trees from each run discarded as burn-in. The maximum clade credibility tree, with median and 95% highest posterior density of divergence times, was estimated with TreeAnnotator v1.8.0[31] (Supplementary Fig. 8). The inferred age of the root was close to 280 million years, a result consistent with recent analyses[13, 32].

Analyses were performed on the EDB lab (Toulouse, France) High Performance Computing system.

## Supplementary References


1. Comte, L., Grenouillet, G. Do stream fish track climate change? Assessing distribution shifts in recent decades across France. *Ecography* **36,** 1236–1246 (2013).

2. Hijmans, R. J., Cameron, S. E., Parra, J. L., Jones, P. G., Jarvis, A. Very high resolution interpolated climate surfaces for global land areas. *International Journal of Climatology* **25,** 1965-1978 (2005).

3. Vogt, J., *et al.* A pan-European river and catchment database In: *Report EUR 22920 EN* (eds European Commission - Joint Research Centre) (2007).

4. Kottelat, M., Freyhof, J. Handbook of European freshwater fishes. (eds Kottelat C., Switzerland and Freyhof) (2007).

5. Deutsch, C. A., *et al.* Impacts of climate warming on terrestrial ectotherms across latitude. *Proc. Natl. Acad. Sci. USA* **105,** 6668-6672 (2008).

6. Clavero, M. Assessing the risk of freshwater fish introductions into the Iberian Peninsula. *Freshw. Biol.* **56,** 2145-2155 (2011).

7. Elliott, A. A comparison of thermal polygons for British freshwater teleosts. *Freshw. Forum* **5,** 178-184 (1995).

8. Elliott, J. M. Some aspects of thermal stress on freshwater teleosts. In: *Stress and fish* (eds Pickering A. D.). Academic Press (1981).

9. Tissot, L., Souchon, Y. Synthesis on thermal tolerances of the principal freshwater fish species of large Western Europe rivers. *Hydroécologie Appliquée* **17,** 17-76 (2010).

10. Poulet, N., Beaulaton, L., Dembski, S. Time trends in fish populations in metropolitan France: insights from national monitoring data. *J. Fish Biol.* **79,** 1436-1452 (2011).

11. Poff, N. L., Allan, J. D. Functional organization of stream fish assemblages in relation to hydrological variability. *Ecology* **76,** 606-627 (1995).

12. Doledec, S., Chessel, D., Grimaret-Carpentier, C. Niche separation in community analysis: a new method. *Ecology* **81,** 2914-2927 (2000).

13. Betancur-R. R, *et al.* The tree of life and a new classification of bony fishes. *PLOS Currents Tree of Life***,** April 18 (2013).

14. Judge, G. G., Griffiths, W. E., Hill, R. C., Lütkepohl, H., Lee, T.-C. *The theory and practice of econometrics*, Second Edition edn. John Wiley & Sons (1985).

15. Le Moigne, P. Description de l'analyse des champs de surface sur la France par le système SAFRAN -Technical report. (eds Centre National de Recherches Météorologiques - Météo-France) (2002).

16. Isaak, D. J., Rieman, B. E. Stream isotherm shifts from climate change and implications for distributions of ectothermic organisms. *Glob. Change Biol.* **19,** 742-751 (2013).

17. Araùjo, M. B., New, M. Ensemble forecasting of species distributions. *Trends Ecol. Evol.* **22,** 42-47 (2007).

18. Quinn, R. M., Gaston, K. J., Arnold, H. R. Relative measures of geographic range size: empirical comparisons. *Oecologia* **107,** 179-188 (1996).

19. Nenzén, H. K., Araùjo, M. B. Choice of threshold alters projections of species range shifts under climate change. *Ecol. Model.* **122,** 3346-3354 (2011).

20. McNamee, R. Regression modelling and other methods to control confounding. *Occup. Environ. Med.* **62,** 500-506 (2005).

21. Edgar, R. C. MUSCLE: a multiple sequence alignment with high accuracy and high throughput. *Nucleic Acids Res.* **32,** 1792-1797 (2004).

22. Misof, B., Misof, K. A Monte Carlo approach successfully identifies randomness in multiple sequence alignments: a more objective means of data exclusion. *Syst. Biol.* **58,** 21-34 (2009).

23. Capella-Gutiérrez, S., Silla-Martínez, J. M., Gabaldón, T. trimAl: a tool for automated alignment trimming in large-scale phylogenetic analyses. *Bioinformatics* **25,** 1972-1973 (2009).

24. Abascal, F., Zardoya, R., Telford, M. J. TranslatorX: multiple alignment of nucleotide sequences guided by amino acid translations. *Nucleic Acids Res.* **38,** (2010).

25. Jeffroy, O., Brinkmann, H., Delsuc, F., Philippe, H. Phylogenomics: the beginning of incongruence? *Trends Genet.* **22,** 225-231 (2006).

26. Paradis, E., Claude, J., Strimmer, K. APE: analyses of phylogenetics and evolution in R language. *Bioinformatics* **20,** 289-290 (2004).

27. Kimura, M. A simple method for estimating evolutionary rate of base substitutions through comparative studies of nucleotide sequences. *J. Mol. Evol.* **16,** 111-120 (1980).

28. Lanfear, R., Calcott, B., Ho, S. Y. W., Guindon, S. PartitionFinder: combined selection of partitioning schemes and substitution models for phylogenetic analyses. *Mol. Biol. Evol.* **29,** 1695-1701 (2012).

29. Drummond, A. J., Rambaut, A. BEAST: Bayesien evolutionary analysis by sampling trees. *BMC Evol. Biol.* **7,** 214 (2007).

30. Burridge, C. P., Craw, D., Fletcher, D., Waters, J. M. Geological dates and molecular rates: fish DNA sheds light on time dependency. *Mol. Biol. Evol.* **25,** 624-633 (2008).

31. Drummond, A. J., Suchard, M. A., Xie, D., Rambaut, A. Bayesian phylogenetics with BEAUti and the BEAST 1.7. *Mol. Biol. Evol.* **29,** 1969-1973 (2012).

32. Broughton, R. E., Betancur-R., R., C. Li, G. Arratia, Ortí, G. Multi-locus phylogenetic analysis reveals the pattern and tempo of bony fish evolution. *PLoS Currents Tree of Life***,** April 16 (2013).